LUND UNIVERSITY

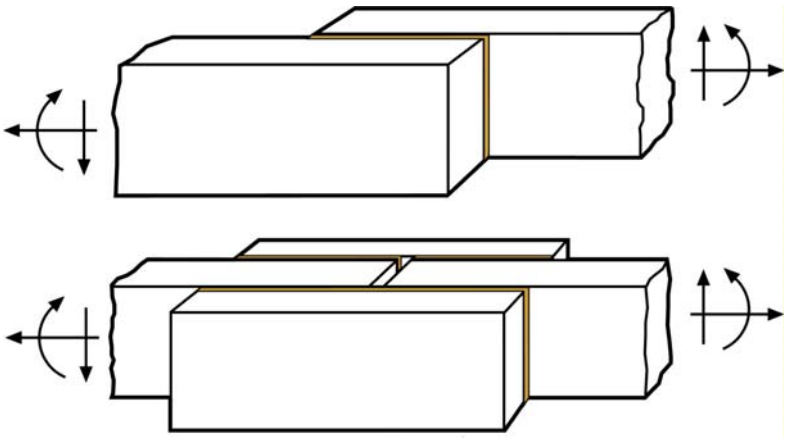

STRESS EQUATIONS FOR 2D LAP JOINTS WITH A COMPLIANT ELASTIC BOND LAYER

PER JOHAN GUSTAFSSON

Structural Mechanics

Department of Construction Sciences
Structural Mechanics

ISRN LUTVDG/TVSM--08/7148--SE (1-43)
ISSN 0281-6679

STRESS EQUATIONS FOR 2D LAP JOINTS WITH A COMPLIANT ELASTIC BOND LAYER

PER JOHAN GUSTAFSSON

Printed by KFS i Lund AB, Lund, Sweden, May 2008.

For information, address:
Division of Structural Mechanics, LTH, Lund University, Box 118, SE-221 00 Lund, Sweden.
Homepage: http://www.byggmek.lth.se

Table of contents

Summary

Explicit formulas were developed for the stress in lap joints loaded in-plane by normal force, shear force and edge-wise bending, giving shear stress in the bond layer. The bond layer material was assumed to be linear elastic with equal or different shear stiffness in the two principal directions of the joint. The two adherends were assumed to act as rigid bodies. By these assumptions were equations for the shear stresses τ_{xz} and τ_{yz} in the bond layer developed, the z-axis being normal to the bond area. The global stiffness properties of a joint were also determined.

Explicit equations for the stresses σ_x, τ_{xy} and σ_y in the adherend material were determined by means equations of equilibrium and by assuming linear variation of the normal stress σ_x with respect to y, i.e. the same variation as assumed in conventional beam theory.

Knowing the stress fields for the stresses in the bond layer and in the adherends, also the maximum stresses were determined, making it possible to formulate failure criteria and identify different joint failure modes. With strength properties typical for wood adherends and a glue bond layer it was for joints exposed to bending found that bond failure was decisive only for very short joints, i.e. for joints with a small length to height ratio. For joints with intermediate length to height ratios were the adherend material modes of failure and the corresponding stress components decisive: the shear stress τ_{xy}, the rolling shear stress τ_{yz} and/or the tension perpendicular to grain σ_y. The normal stress σ_x is decisive for the full bending moment capacity of the adherends. This capacity was reached for long joints.

The accuracy of the stress equations were studied by means of plane stress finite element analysis, taking into account linear elastic deformations of the adherends. It was found that the assumption of linear variation of the normal stress σ_x with respect to y is reasonable. The assumption of rigid adherend performance was studied by identifying a dimensionless adherend rigidity ratio, which for joints with an isotropic adherend material is $Ebt/(Ga^2)$ where E, b and a represents the Young's modulus, thickness and length, respectively, of the adherends, and t and G the thickness and the shear modulus, respectively, of the bond layer material. Good accuracy was for found for joints made up of steel adherends joined by means of a rubber foil glued between the steel parts. For corresponding rubber foil adhesive joints with wood adherends was good accuary found for joints of small size.

1. Introduction

Lap joints of the kind shown Figure 1 are considered. The adherends can be made of wood, steel or any other reasonably stiff structural material. In the analysis it is assumed that the adhered material is very stiff as compared to the bond layer material. The bond layer is assumed to compliant with a linear elastic isotropic or orthotropic performance. It can for instance be made up of a rubber foil glued in between the two adherends. The results obtained might be applicable also to nailed joints and punched metal plate nail fastener joints with a large number of nails so that their action can be approximated with distributed shear stress.

Only the in-plane performance of joints with a rectangular bond area is considered. The analysis is thus 2D and relates to the stress components σ_x, σ_y and τ_{xy} in the adherends and to the out-of-plane shear stress components τ_{xz} and τ_{yz} in the bond layer, and to the joint strength as limited by the magnitude of these stress components. It is in analogy with beam theory analysis assumed that the variation of the normal stress σ_x is linear with respect to y. The below derivations are carried out with reference to a single lap joint, Figure 1a), but the results are valid also for double lap joints and pairs of double lap joints, Figure 1 b).

Method for calculation of the 3D stiffness and bond layer stress components in lap joints has been dealt with in (Gustafson, 2006). The purpose of the present study is to find equations for simple calculation of the adherend stresses σ_x, σ_y and τ_{xy} in the joint area. Experimental tests of various wood material lap joints joined with a flexible bond layer have shown that fracture in the wood corresponding to the stress components σ_x, σ_y and/or τ_{xy} often is decisive for the load carrying capacity. The calculated stresses are approximate as a result of the assumptions of rigid adherend performance and linear variation of σ_x with respect to y. Experimental results are available in (Gustafsson, 2007) and (Björnsson and Danielsson, 2005) for rubber foil glued lap joints glulam-to-glulam, LVL-to-glulam, wood-to-wood and glulam-to-steel.

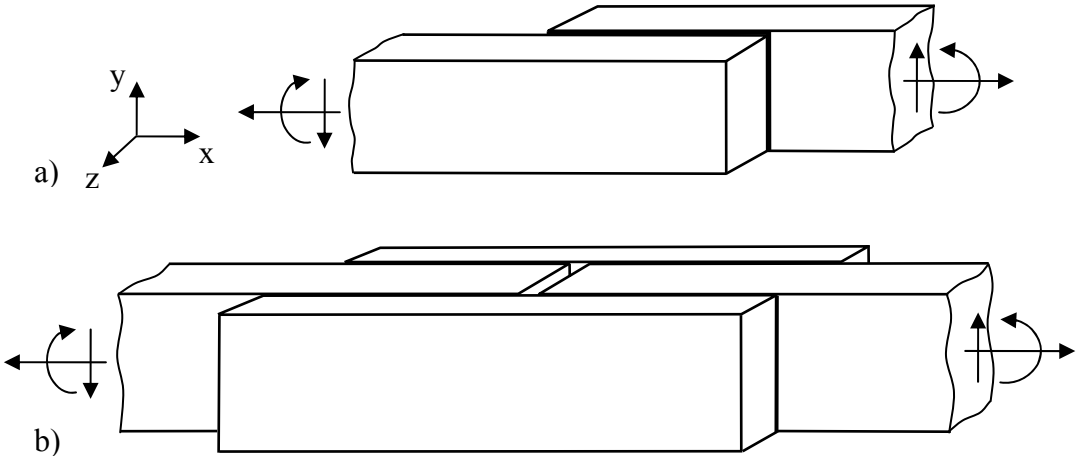

Figure 1. Example of lap joints: a) with a single lap and, b), with two double laps.

2. Bond layer shear stress and joint stiffness

2.1 Notations and assumptions

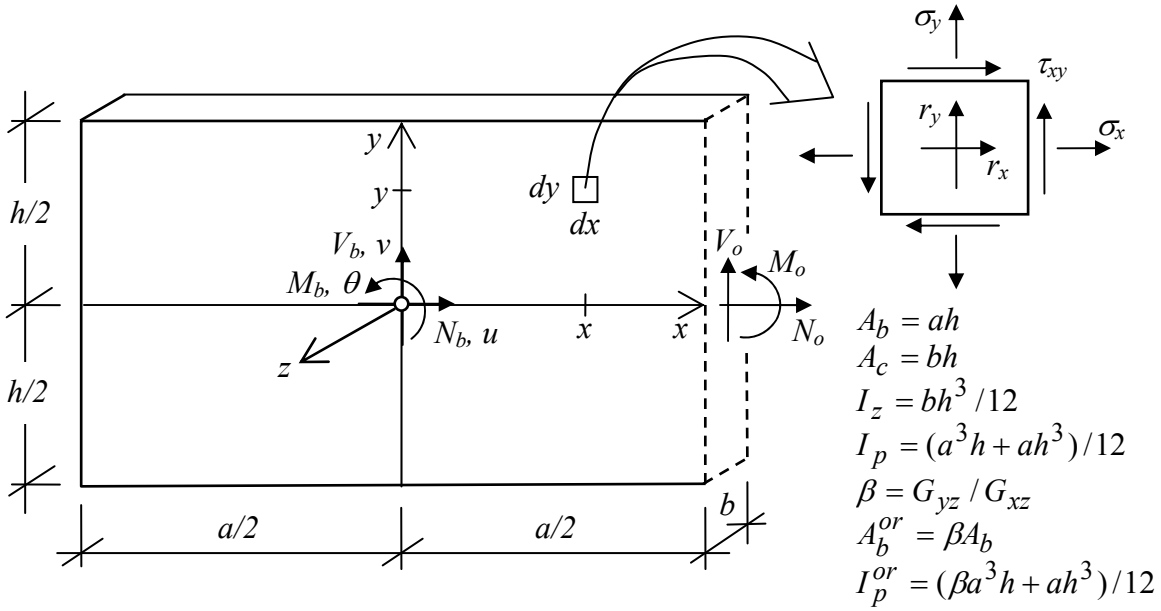

Figure 2. Back adherend of the joint in Figure 1a) with notations.

Notations and measures of an adherend are shown in Figure 2. The thickness of the bond layer is denoted *t*. The bond area is a rectangle, *ah*, and the adherend is a cuboid, *ahb*. The bond layer shear stresses τ_{xz} and τ_{yz}, and the global joint stiffness are calculated at the following assumptions:

- Rigid performance of the adherends
- Relative movement between the two adherends only in the *x*-*y* plane, i.e. 2D analysis
- Linear elastic isotropic or orthotropic properties of the bond layer
- Constant shear strain and stress in the bond layer across the thickness *t* of the layer, i.e. constant τ_{xz} and τ_{yz} with respect to *z*

The cases isotropic and orthotropic stiffness of the bond layer are both dealt with. The isotropic shear modulus is denoted *G*, and the orthotropic shear moduli are denoted G_{xz} and G_{yz}. The case of orthotropic shear stiffness of the bond layer is of interest in the case of wood adherends since the out-of-plane shear deformations of the adherends in an approximate manner can be considered by including them in the bond layer compliance.

2.2 Isotropic case

The assumptions made in Section 2.1 imply for the case of isotropic bond layer properties that

$$\begin{bmatrix}\tau_{xz}\\ \tau_{yz}\end{bmatrix} = G/t\begin{bmatrix}\Delta u - y\Delta\theta\\ \Delta v + x\Delta\theta\end{bmatrix} = G/t\begin{bmatrix}1 & 0 & -y\\ 0 & 1 & x\end{bmatrix}\begin{bmatrix}\Delta u\\ \Delta v\\ \Delta\theta\end{bmatrix} \tag{1}$$

where Δu, Δv and $\Delta\theta$ indicate the relative rigid body movement between the two adherends with the centre of the bond area as point of reference as indicated in Figure 2:

$$\begin{bmatrix}\Delta u\\ \Delta v\\ \Delta\theta\end{bmatrix} = \begin{bmatrix}u\\ v\\ \theta\end{bmatrix}_{front} - \begin{bmatrix}u\\ v\\ \theta\end{bmatrix}_{back} \tag{2}$$

The surface loads r_x and r_y acting on the back adherend are by the law of action and reaction equal to the bond layer shear stresses:

$$\begin{bmatrix}r_x\\ r_y\end{bmatrix} = \begin{bmatrix}\tau_{xz}\\ \tau_{yz}\end{bmatrix} \tag{3}$$

The force and moment actions that are statically equivalent to the surface loads are obtained from Eq. (1) by integration:

$$\begin{bmatrix}N_b\\ V_b\\ M_b\end{bmatrix} = \int_{A_b}\begin{bmatrix}r_x\\ r_y\\ xr_y - yr_x\end{bmatrix}dA = G/t\begin{bmatrix}A_b & 0 & 0\\ 0 & A_b & 0\\ 0 & 0 & I_p\end{bmatrix}\begin{bmatrix}\Delta u\\ \Delta v\\ \Delta\theta\end{bmatrix} \tag{4}$$

This equation gives the stiffness of the joint with the centre of the bond area as point of reference. A_b is the bond area and I_p is the polar moment of inertia of the bond area as defined in Figure 2. Equilibrium of the adherend relates the surface load action to the cross section forces and moments:

$$\begin{bmatrix}N_b\\ V_b\\ M_b\end{bmatrix} = \begin{bmatrix}-1 & 0 & 0\\ 0 & -1 & 0\\ 0 & -a/2 & -1\end{bmatrix}\begin{bmatrix}N_o\\ V_o\\ M_o\end{bmatrix} \tag{5}$$

Before the calculation of adherend stresses it is convenient to combine (4) and (5) for calculation of the relative displacements from given cross section quantities:

$$\begin{bmatrix}\Delta u\\ \Delta v\\ \Delta\theta\end{bmatrix} = -t/G\begin{bmatrix}1/A_b & 0 & 0\\ 0 & 1/A_b & 0\\ 0 & a/(2I_p) & 1/I_p\end{bmatrix}\begin{bmatrix}N_o\\ V_o\\ M_o\end{bmatrix} \tag{6}$$

Use of Eq. (1) and (3)-(6) gives the following alternative equations for the bond layer shear stresses as a function of the global joint deformation, the surface load actions or the cross section forces and bending moment:

$$\begin{bmatrix}\tau_{xz}\\ \tau_{yz}\end{bmatrix} = \begin{bmatrix}r_x\\ r_y\end{bmatrix} = G/t\begin{bmatrix}1 & 0 & -y\\ 0 & 1 & x\end{bmatrix}\begin{bmatrix}\Delta u\\ \Delta v\\ \Delta\theta\end{bmatrix} =$$

$$= \begin{bmatrix}\frac{1}{A_b} & 0 & \frac{-y}{I_p}\\ 0 & \frac{1}{A_b} & \frac{x}{I_p}\end{bmatrix}\begin{bmatrix}N_b\\ V_b\\ M_b\end{bmatrix} = \begin{bmatrix}\frac{-1}{A_b} & \frac{ay}{2I_p} & \frac{y}{I_p}\\ 0 & -\frac{1}{A_b}-\frac{ax}{2I_p} & \frac{-x}{I_p}\end{bmatrix}\begin{bmatrix}N_o\\ V_o\\ M_o\end{bmatrix} \tag{7}$$

The total bond layer shear stress, τ_b, is:

$$\tau_b = \sqrt{\tau_{xz}^2+\tau_{yz}^2} = G/t\sqrt{(\Delta u - y\Delta\theta)^2+(\Delta v + x\Delta\theta)^2} =$$

$$= \sqrt{\frac{N_b^2}{A_b^2}+\frac{V_b^2}{A_b^2}+\frac{M_b^2}{I_p^2}(x^2+y^2)+\frac{2M_b}{A_bI_p}(xV_b-yN_b)} = \tag{8}$$

$$= \sqrt{\frac{N_o^2}{A_b^2}+\frac{V_o^2}{A_b^2}+\frac{(M_o+V_oa/2)^2}{I_p^2}(x^2+y^2)+\frac{2(M_o+V_oa/2)}{A_bI_p}(xV_o-yN_o)}$$

2.3 Orthotropic case

For orthotropic stiffness properties of the bond layer is

$$\begin{bmatrix}\tau_{xz}\\ \tau_{yz}\end{bmatrix} = \begin{bmatrix}(G_{xz}/t)(\Delta u - y\Delta\theta)\\ (G_{yz}/t)(\Delta v + x\Delta\theta)\end{bmatrix} = G_{xz}/t\begin{bmatrix}(\Delta u - y\Delta\theta)\\ \beta(\Delta v + x\Delta\theta)\end{bmatrix} = G_{xz}/t\begin{bmatrix}1 & 0 & -y\\ 0 & \beta & \beta x\end{bmatrix}\begin{bmatrix}\Delta u\\ \Delta v\\ \Delta\theta\end{bmatrix} \tag{9}$$

where $\beta=G_{yz}/G_{xz}$. Analysis in analogy with the analysis for isotropic bond layer stiffness gives the joint stiffness as

$$\begin{bmatrix} N_b \\ V_b \\ M_b \end{bmatrix} = G_{xz}/t \begin{bmatrix} A_b & 0 & 0 \\ 0 & A_b^{or} & 0 \\ 0 & 0 & I_p^{or} \end{bmatrix} \begin{bmatrix} \Delta u \\ \Delta v \\ \Delta\theta \end{bmatrix} \tag{10}$$

where A_b^{or} and I_p^{or} are defined in Figure 2. The orthotropic correspondence to Eq. (6) becomes

$$\begin{bmatrix} \Delta u \\ \Delta v \\ \Delta\theta \end{bmatrix} = -t/G_{xz} \begin{bmatrix} 1/A_b & 0 & 0 \\ 0 & 1/A_b^{or} & 0 \\ 0 & a/(2I_p^{or}) & 1/I_p^{or} \end{bmatrix} \begin{bmatrix} N_o \\ V_o \\ M_o \end{bmatrix} \tag{11}$$

which gives the following alternative equations for the bond layer shear stresses and for the surface load acting on the adherend:

$$\begin{bmatrix} \tau_{xz} \\ \tau_{yz} \end{bmatrix} = \begin{bmatrix} r_x \\ r_y \end{bmatrix} = G_{xz}/t \begin{bmatrix} 1 & 0 & -y \\ 0 & \beta & \beta x \end{bmatrix} \begin{bmatrix} \Delta u \\ \Delta v \\ \Delta\theta \end{bmatrix} =$$

$$= \begin{bmatrix} \frac{1}{A_b} & 0 & \frac{-y}{I_p^{or}} \\ 0 & \frac{1}{A_b} & \frac{\beta x}{I_p^{or}} \end{bmatrix} \begin{bmatrix} N_b \\ V_b \\ M_b \end{bmatrix} = \begin{bmatrix} \frac{-1}{A_b} & \frac{ay}{2I_p^{or}} & \frac{y}{I_p^{or}} \\ 0 & -\frac{1}{A_b} - \frac{\beta a x}{2I_p^{or}} & \frac{-\beta x}{I_p^{or}} \end{bmatrix} \begin{bmatrix} N_o \\ V_o \\ M_o \end{bmatrix} \tag{12}$$

The alternative equations for the total shear stress of an orthotropic bond layer becomes

$$\tau_b = \sqrt{\tau_{xz}^2 + \tau_{yz}^2} = G_{xz}/t\sqrt{(\Delta u - y\Delta\theta)^2 + \beta^2(\Delta v + x\Delta\theta)^2} =$$

$$= \sqrt{\frac{N_b^2}{A_b^2} + \frac{V_b^2}{A_b^2} + \frac{M_b^2}{(I_p^{or})^2}(\beta^2 x^2 + y^2) + \frac{2M_b}{A_b I_p^{or}}(\beta x V_b - y N_b)} = \tag{13}$$

$$= \sqrt{\frac{N_o^2}{A_b^2} + \frac{V_o^2}{A_b^2} + \frac{(M_o + V_o a/2)^2}{(I_p^{or})^2}(\beta^2 x^2 + y^2) + \frac{2(M_o + V_o a/2)}{A_b I_p^{or}}(\beta x V_o - y N_o)}$$

2.4 Illustration of bond layer shear stress distribution

Isotropic bond layer, β=1.0 Orthotropic bond layer, β=0.25

τ_{xz} max/min: 4.10/-4.10 MPa

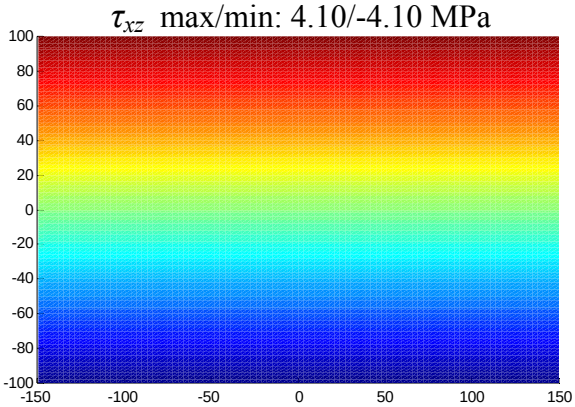

τ_{xz} max/min: 8.53/-8.53 MPa

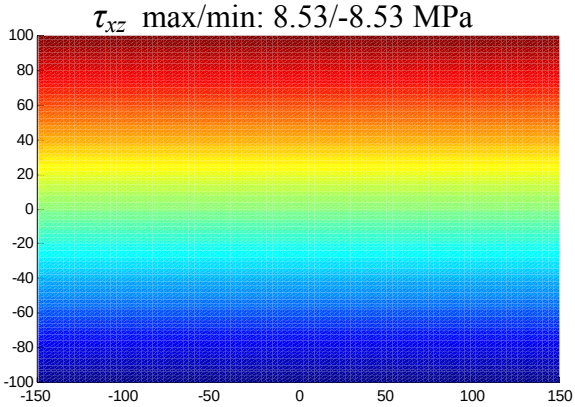

τ_{yz} max/min: 6.15/-6.15 MPa

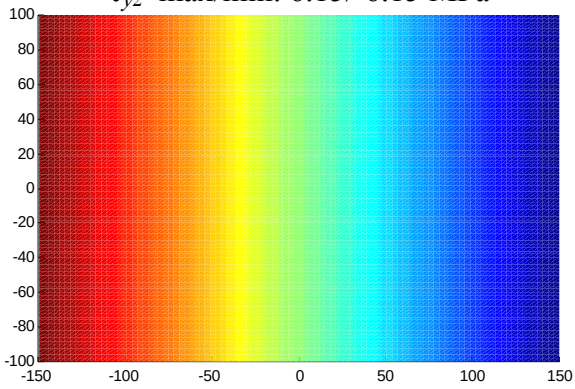

τ_{yz} max/min: 3.20/-3.20 MPa

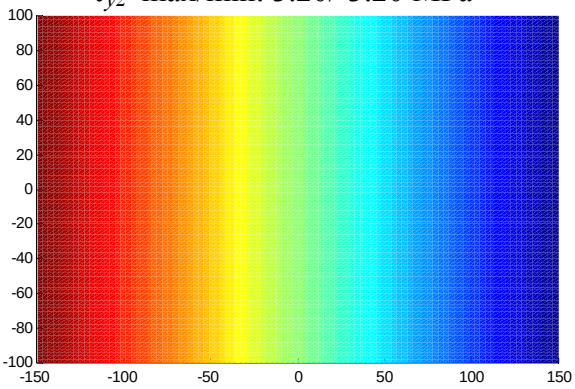

τ_b, max/min: 7.40/0.00 MPa

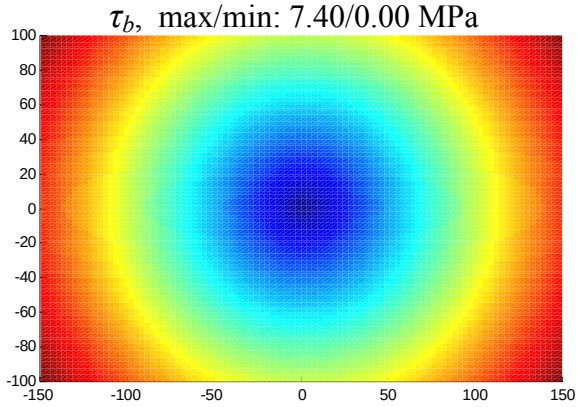

τ_b, max/min: 9.11/0.00 MPa

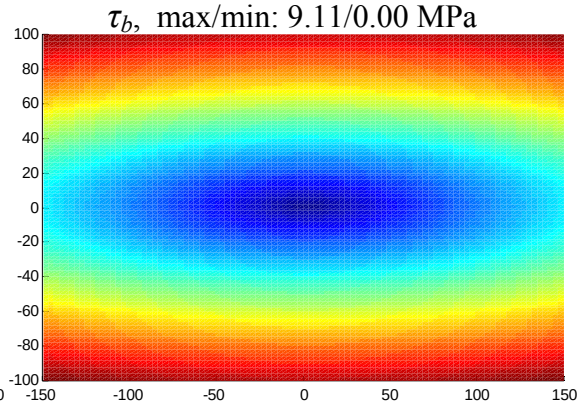

The above illustrations of calculated distribution and magnitude of the shear stresses in an isotropic and an orthotropic bond layer are valid for a joint with length a=300 mm and height h=200 mm loaded by a pure bending moment M_o=26.67 kNm. The calculations were made by means Eq. (12) and (13). Red color indicates positive shear stress and dark blue color negative or zero shear stress. The bending moment 26.67 kNm corresponds to the bending stress 40 MPa for beam cross section of height 200 mm and width 100 mm.

3. Adherend stress analysis

3.1 Assumptions

The adherend stresses σ_x, σ_y and τ_{xy} are derived by means of two assumptions and by use of equations of equilibrium and static equivalence. The first assumption is that the surface loads r_x and r_y are according to Eq. (7) for the isotropic case and according to (12) for the orthotropic case. Eq. (7) and (12) were obtained from the assumption listed in Section 2.1 and are thus accurate if the adherends are stiff and the bond layer is linear elastic and reasonably thin. The second assumption is that the normal stress σ_x has a linear variation with respect to y, i.e. that

$$\sigma_x(x,y) = C_1(x) + C_2(x)y \tag{14}$$

The linear variation of $\sigma_x(y)$ is in accordance with the Bernoulli-Euler and Timoshenko beam theories. No assumption is made with respect to the properties of the adherend material. However, the assumptions of linear $\sigma_x(y)$ and surface loading according to Eq. (7) or (12) suggests that the analysis relates primarily to adherends that are linear elastic and stiff as compared to stiffness of the bond layer.

The stresses σ_x, σ_y and τ_{xy} can now be determined from the equations of equilibrium for a plate,

$$\begin{cases} \dfrac{\partial \sigma_x}{\partial x} + \dfrac{\partial \tau_{xy}}{\partial y} + \dfrac{r_x}{b} = 0 \\ \dfrac{\partial \sigma_y}{\partial y} + \dfrac{\partial \tau_{xy}}{\partial x} + \dfrac{r_y}{b} = 0 \end{cases} \tag{15}$$

, together with the boundary conditions indicated in Figure 2: i.e. three edges where the edge tractions are zero and one edge where the integrated action of σ_x is statically equivalent with the cross section loads N_o and M_o, and the integrated action of τ_{xy} is statically equivalent with V_o.

In the below are the equilibrium and static equivalence calculations carried out in steps in analogy with beam theory analysis so that distributed beam load and also the cross section bending moment, normal force and shear force are obtained as intermediate results.

3.2 Adherend line loads

The surface loads r_x and r_y acting on the adherend can by static equivalence be expressed as force and moment line loads q_x, q_y and m_z acting on the line y=0:

$$\begin{bmatrix} q_x \\ q_y \\ m_z \end{bmatrix} = \int_{-h/2}^{h/2} \begin{bmatrix} r_x \\ r_y \\ -yr_x \end{bmatrix} dy = \frac{Gh}{t} \begin{bmatrix} 1 & 0 & 0 \\ 0 & 1 & x \\ 0 & 0 & h^2/12 \end{bmatrix} \begin{bmatrix} \Delta u \\ \Delta v \\ \Delta\theta \end{bmatrix} =$$
$$= \frac{-h}{12 I_p} \begin{bmatrix} h^2 + a^2 & 0 & 0 \\ 0 & h^2 + a^2 + 6ax & 12x \\ 0 & h^2 a/2 & h^2 \end{bmatrix} \begin{bmatrix} N_o \\ V_o \\ M_o \end{bmatrix} \quad (16)$$

The above result is valid for the isotropic case. The orthotropic case gives

$$\begin{bmatrix} q_x \\ q_y \\ m_z \end{bmatrix} = \int_{-h/2}^{h/2} \begin{bmatrix} r_x \\ r_y \\ -yr_x \end{bmatrix} dy = \frac{G_{xz} h}{t} \begin{bmatrix} 1 & 0 & 0 \\ 0 & \beta & \beta x \\ 0 & 0 & h^2/12 \end{bmatrix} \begin{bmatrix} \Delta u \\ \Delta v \\ \Delta\theta \end{bmatrix} =$$
$$= \frac{-h}{12 I_p^{or}} \begin{bmatrix} h^2 + \beta a^2 & 0 & 0 \\ 0 & h^2 + \beta a^2 + 6\beta ax & 12\beta x \\ 0 & h^2 a/2 & h^2 \end{bmatrix} \begin{bmatrix} N_o \\ V_o \\ M_o \end{bmatrix} \quad (17)$$

3.3 Adherend cross-section forces and moment

The cross section forces and moment acting on the part to the left of a cross section located at x are obtained by equations of equilibrium. The action of the line loads is calculated by integration from $x=-a/2$ to $x=x$. For the isotropic case, the equations of equilibrium give:

$$\begin{bmatrix} N(x) \\ V(x) \\ M(x) \end{bmatrix} = \int_{-a/2}^{x} \begin{bmatrix} -q_x(s) \\ -q_y(s) \\ q_y(s)(x-s) - m_z(s) \end{bmatrix} ds = \tag{18}$$

$$= \frac{-Gh\ (x+a/2)}{t} \begin{bmatrix} 1 & 0 & 0 \\ 0 & 1 & (x-a/2)/2 \\ 0 & -(x+a/2)/2 & (a^2+h^2)/12 - x(x-a/2)/6 \end{bmatrix} \begin{bmatrix} \Delta u \\ \Delta v \\ \Delta\theta \end{bmatrix} =$$

$$= \frac{x+a/2}{h^2 a + a^3} \begin{bmatrix} h^2+a^2 & 0 & 0 \\ 0 & h^2+a^2+3a(x-a/2) & 6(x-a/2) \\ 0 & (-h^2/2 - a^2/2 - ax)(x-a/2) & h^2+a^2-2x(x-a/2) \end{bmatrix} \begin{bmatrix} N_o \\ V_o \\ M_o \end{bmatrix}$$

The relation $V=dM/dx$, often cited in textbooks, is not valid in this case because of the non-zero bending moment line load m_z.

For the orthotropic case, i.e. for $\beta \neq 1$, is found:

$$\begin{bmatrix} N(x) \\ V(x) \\ M(x) \end{bmatrix} = \int_{-a/2}^{x} \begin{bmatrix} -q_x(s) \\ -q_y(s) \\ q_y(s)(x-s) - m_z(s) \end{bmatrix} ds = \tag{19}$$

$$= \frac{-G_{xz} h\ (x+a/2)}{t} \begin{bmatrix} 1 & 0 & 0 \\ 0 & \beta & \beta(x-a/2)/2 \\ 0 & -\beta(x+a/2)/2 & (\beta a^2+h^2)/12 - \beta x(x-a/2)/6 \end{bmatrix} \begin{bmatrix} \Delta u \\ \Delta v \\ \Delta\theta \end{bmatrix} =$$

$$= \frac{h(x+a/2)}{12 I_p^{or}} \ldots$$

$$\begin{bmatrix} h^2+a^2 & 0 & 0 \\ 0 & h^2+\beta a^2+3\beta a(x-a/2) & 6\beta(x-a/2) \\ 0 & (-h^2/2 - \beta a^2/2 - \beta ax)(x-a/2) & h^2+\beta a^2-2\beta x(x-a/2) \end{bmatrix} \begin{bmatrix} N_o \\ V_o \\ M_o \end{bmatrix}$$

3.4 Normal stress σ_x

Due to the assumption if linear distribution of σ_x with respect to y, σ_x can be calculated in the same way as by conventional beam theory:

$$\sigma_x = \frac{N(x)}{A_c} - \frac{M(x)\,y}{I_z} \tag{20}$$

where $A_c=bh$ is the cross-section area and $I_z=bh^3/12$ is the moment of inertia of the cross-section. With $N(x)$ and $M(x)$ from Eq. (18), the normal stress σ_x in point (x,y) is for the isotropic case found to be

$$\begin{aligned}\sigma_x = & \frac{(2x+a)}{2abh}\, N_o + \\ & + \frac{(h^2+a^2+2ax)(4x^2-a^2)\,hy}{96 I_z I_p}\, V_o + \\ & + \frac{(-h^2-a^2+2x^2-ax)(2x+a)\,hy}{24 I_z I_p}\, M_o\end{aligned} \tag{21}$$

The orthotropic case gives

$$\begin{aligned}\sigma_x = & \frac{(2x+a)}{2abh}\, N_o + \\ & + \frac{(h^2+\beta a^2+2\beta ax)(4x^2-a^2)\,hy}{96 I_z I_p^{or}}\, V_o + \\ & + \frac{(-h^2-\beta a^2+2\beta x^2-\beta ax)(2x+a)\,hy}{24 I_z I_p^{or}}\, M_o\end{aligned} \tag{22}$$

3.5 Shear stress τ_{xy}

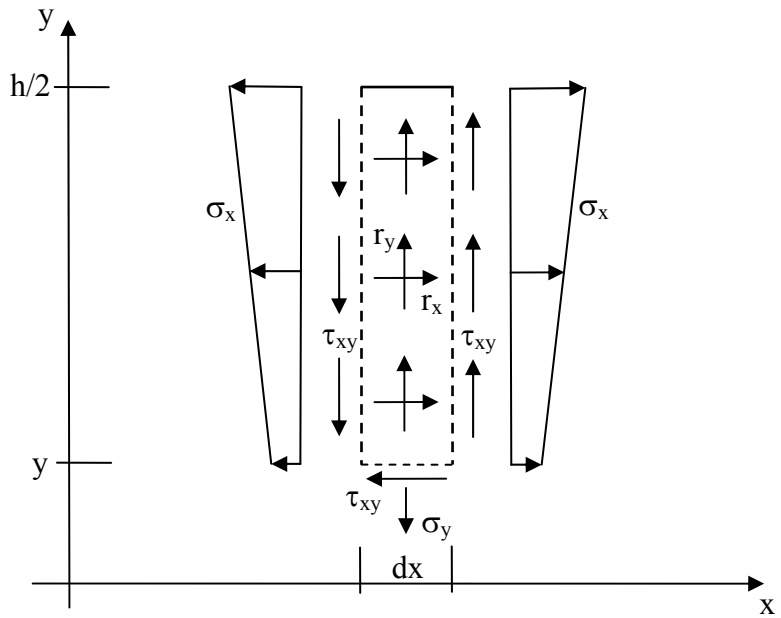

Figure 3. Free body diagram of a part (*h/2-y*)*dx* of an adherend.

The shear stress τ_{xy} in a point (*x,y*) is found by equilibrium of the horizontal forces acting on a strip (*h/2-y*)*dx* of the adherend shown in Figure 3:

$$\int_y^{h/2} (\sigma_x(x+dx) - \sigma_x(x))\,b dy + \int_y^{h/2} r_x dx dy - \tau_{xy} b dx = 0 \tag{23}$$

By dividing all terms by *dx* and noting that

$$\frac{\sigma_x(x+dx) - \sigma_x(x)}{dx} = \frac{d\sigma_x}{dx} \ , \tag{24}$$

it is for the isotropic case by use of the expressions for r_x and σ_x given by Eq. (7) and (21) found that

$$\tau_{xy} = \frac{((h^2 + a^2)(4x + 2a) \ + \ 3a(4x^2 - a^2))(h^3 - 4hy^2)}{384 I_z I_p} \ V_o \ + \\ + \ \frac{(4x^2 - a^2)(h^3 - 4hy^2)}{64 I_z I_p} \ M_o \tag{25}$$

For the case of an orthotropic bond layer, the shear stress is:

$$\tau_{xy} = \frac{((h^2+\beta a^2)(4x+2a) \; + \; 3\beta a(4x^2-a^2))(h^3-4hy^2)}{384 I_z I_p^{or}} \; V_o \; + \\ + \; \frac{\beta(4x^2-a^2)(h^3-4hy^2)}{64 I_z I_p^{or}} \; M_o \tag{26}$$

3.6 Normal stress σ_y

The normal stress σ_y in a point (x,y) is determined by equilibrium of the vertical forces acting on the strip $(h/2\text{-}y)dx$ shown in Figure 3:

$$\int_y^{h/2} (\tau_{xy}(x+dx) - \tau_{xy}(x)) b dy + \int_y^{h/2} r_y dx dy - \sigma_y b dx = 0 \tag{27}$$

Dividing all terms by dx and with $(\tau_{xy}(x+dx) - \tau_{xy}(x))/dx = d\tau_{xy}/dx$, it is by use of Eq. (7) and (25) for the isotropic case found that

$$\sigma_y = \frac{(h^2+a^2+6ax)\,(4hy^3-h^3y)}{288\, I_z I_p} \; V_o \; + \; \frac{x\,(4hy^3-h^3y)}{24\, I_z I_p} \; M_o \tag{28}$$

and for the orthotropic case that

$$\sigma_y = \frac{(h^2+\beta a^2+6\beta ax)\,(4hy^3-h^3y)}{288\, I_z I_p^{or}} \; V_o \; + \; \frac{\beta x\,(4hy^3-h^3y)}{24\, I_z I_p^{or}} \; M_o \tag{29}$$

3.7 Verification of stress formulas

The equations for the stresses σ_x, τ_{xy}, and σ_y i.e. Eq. (21) and (22), (25) and (26), and (28) and (29), must fulfill the two differential equations of equilibrium and the boundary conditions:

- fulfill Eq. (15) for all x and y, for all values N_o, V_o and M_o
- give $\sigma_x = \tau_{xy} = 0$ for $x=-a/2$
- give $\sigma_y = \tau_{xy} = 0$ for $y=\pm h/2$
- and for $x=a/2$ give

$$\int_{-h/2}^{h/2} \sigma_x b dy = N_o, \quad \int_{-h/2}^{h/2} -y\sigma_x b dy = M_o \quad \textit{and} \quad \int_{-h/2}^{h/2} \tau_{xy} b dy = V_o \tag{30}$$

These conditions can be fulfilled by various stress fields. The particular stress solution considered here must moreover fulfill the assumption of linear variation of σ_x with y, i.e. Eq. (14). The above conditions make it possible to check the stress equations.

3.8 Illustration of distribution of stresses in an adherend

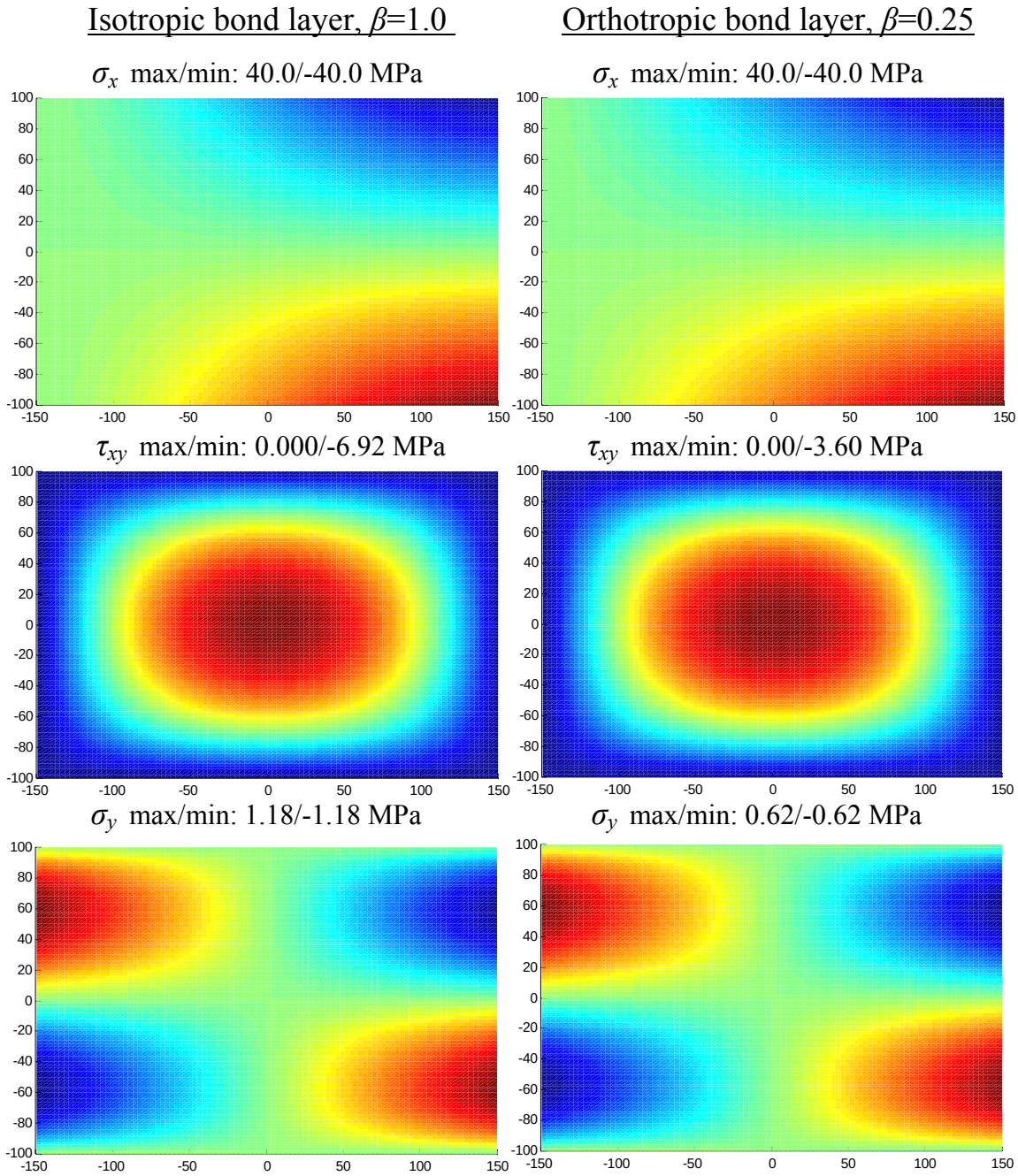

The above illustrations of calculated magnitude and distribution of the in-plane stresses in an adherend for isotropic and an orthotropic bond layer properties are valid for a joint with length a=300 mm and height h=200 mm and adherend thickness b=100 mm loaded by a pure bending moment M_o=26.67 kNm. The calculations are made by means Eq. (22), (26) and (29). Note the different magnitude of the stresses σ_y and τ_{xy} for the isotropic and orthotropic cases, although the shape of the stress distributions are the almost same. For σ_x and σ_y is red color indicating positive stress (tension) and blue color negative stress. For τ_{xy} is red color indicating negative stress and dark blue color zero stress.

4. Magnitude and location of extreme stresses

The bond layer stresses τ_{xz}, τ_{yz} and τ_b and the adherend stresses σ_x, τ_{xy} and σ_y are given by the equations in Sections 2 and 3, respectively. The minimum and maximum of these stresses are of concern in joint strength analysis. The locations and the values of the extremes are for a joint with isotropic bond layer stiffness and exposed to pure bending $M_o=M_b\neq 0$ given in Table 1. For shear force loading, V_o, and normal force loading, N_o, are the location of the extremes shown in Table 2. For orthotropic bond layers can the corresponding results be obtained from the stress equations in Sections 2 and 3.

Table 1. Minimum and maximum of stresses at bending M_o of an isotropic joint .

Stress component	Minimum		Maximum	
	Location, (x,y)	Value	Location, (x,y)	Value
τ_{xz}	$(x,-h/2)$	$\frac{-6M_o}{h^2a+a^3}$	$(x,h/2)$	$\frac{6M_o}{h^2a+a^3}$
τ_{yz}	$(a/2,y)$	$\frac{-6M_o}{h^3+ha^2}$	$(-a/2,y)$	$\frac{6M_o}{h^3+ha^2}$
τ_b	$(0,0)$	0	$(\pm a/2,\pm h/2)$	$\frac{6\sqrt{a^2+h^2}\,M_o}{h^3a+ha^3}$
σ_x	$(a/2,h/2)$	$\frac{-6M_o}{bh^2}$	$(a/2,-h/2)$	$\frac{6M_o}{bh^2}$
τ_{xy}	$(0,0)$	$\frac{-9a^2M_o}{4b(h^3a+ha^3)}$	$(\pm a/2,y)$ $(x,\pm h/2)$	0
σ_y	$(a/2,h/\sqrt{12})$ $(-a/2,-h/\sqrt{12})$	$\frac{-M_o}{\sqrt{3}\,b(a^2+h^2)}$	$(a/2,-h/\sqrt{12})$ $(-a/2,h/\sqrt{12})$	$\frac{M_o}{\sqrt{3}\,b(a^2+h^2)}$

Table 2. Extreme value location and value at various loading of isotropic joint.

For normal force N_o at $x = a/2$:		
Stress	Locations (x, y)	Value
τ_{xz}	(x, y)	$N_o/(ha)$
τ_{yz}	(x, y)	0
τ_b	(x, y)	$N_o/(ha)$
σ_x	$(a/2, y)$	$N_o/(bh)$
τ_{xy}	(x, y)	0
σ_y	(x, y)	0
For shear force V_o at $x = a/2$:		
Stress	Locations (x, y)	Value
τ_{xz}	$(x, \pm h/2)$	See Eq. 7
τ_{yz}	$(\pm a/2, y)$	See Eq. 7
τ_b	$(\max\{-a/2, -(a^2+h^2)/(6a)\}, 0)$, $(a/2, \pm h/2)$	See Eq. 8
σ_x	$(-(a^2+h^2)/(6a) \pm \sqrt{((a^2+h^2)/(6a))^2 + a^2/12}, \pm h/2)$ *	See Eq. 21
τ_{xy}	$(\max\{-a/2, -(a^2+h^2)/(6a)\}, 0)$	See Eq. 25
σ_y	$(\pm a/2, \pm h/\sqrt{12})$	See Eq. 28
For bending moment M_o at $x = a/2$:		
Stress	Locations (x, y)	Value
τ_{xz}	$(x, \pm h/2)$	See Table 1
τ_{yz}	$(\pm a/2, y)$	See Table 1
τ_b	$(0, 0)$, $(\pm a/2, \pm h/2)$	See Table 1
σ_x	$(a/2, \pm h/2)$	See Table 1
τ_{xy}	$(0, 0)$, $(\pm a/2, y)$, $(x, \pm h/2)$	See Table 1
σ_y	$(\pm a/2, \pm h/\sqrt{12})$	See Table 1

* also $(\pm a/2, \pm h/2)$

5. Joint strength analysis

5.1 Failure criteria

Joint strength is here analyzed at the assumption of joint failure when any of the stress components studied equals the corresponding strength parameter value. Combined failure criteria taking into account several stress components are also possible. The strength properties of the bond layer are regarded as isotropic and the strength properties of the adherend material as orthotropic. The strength parameter notation is the notation commonly used for wood. With the present joint failure criterion, the joint is predicted to fail when any of the following criteria (a)-(f) is fulfilled:

(a) Bond layer failure:

$$\tau_b = f_{v,b} \tag{31}$$

The value of $f_{v,b}$ may for instance reflect the shear strength of a rubber layer and the two glue lines between the rubber and the two adherends.

(b) Longitudinal out-of-plane shear stress failure in the adherend in the close vicinity of the adherend-glue interface:

$$|\tau_{xz}| = f_v \tag{32}$$

(c) Rolling shear stress failure in the adherend in the vicinity of the bond line:

$$|\tau_{yz}| = f_{v,r} \tag{33}$$

(d) Normal stress failure in adherend:

$$\sigma_x = \begin{cases} f_{t,0} & \text{for } \sigma_x > 0 \\ -f_{c,0} & \text{for } \sigma_x < 0 \end{cases} \tag{34}$$

This criterion for σ_x follows the assumption of joint failure when any of the stress components equals the corresponding strength value. At strength design of wooden beams in bending and combined bending and normal force is an additional third strength parameter commonly used, namely the so-called bending strength f_m (Larsen and Riberholt, 1999), and an other adherend failure criterion is then used:

$$\begin{cases} \dfrac{\sigma_{xn}}{f_{t,0}} + \dfrac{\sigma_{xm}}{f_m} = 1 & for\ \sigma_{xn} > 0 \\ \dfrac{-\sigma_{xn}}{f_{c,0}} + \dfrac{\sigma_{xm}}{f_m} = 1 & for\ \sigma_{xn} < 0 \end{cases}$$

where $\sigma_{xn} = N/(bh)$ and $\sigma_{xm} = |M_o|/(bh^2/6)$.

(e) Longitudinal in-plane shear stress failure in adherend:

$$|\tau_{xy}| = f_v \tag{35}$$

(f) Perpendicular to the joint normal stress failure in adherend:

$$\sigma_y = \begin{cases} f_{t,90} & \text{for } \sigma_y > 0 \\ -f_{c,90} & \text{for } \sigma_y < 0 \end{cases} \tag{36}$$

5.2 Joint bending strength analysis – isotropic bond layer

A joint exposed only to bending and with an isotropic bond layer is analyzed. The failure modes corresponding to the above criteria (a)-(f) are for this case of loading illustrated in Figure 4.

The full bending moment capacity of the joint is determined by bending failure of the adherends. This moment is given by criteria (d) and denoted M_m:

$$M_m = \frac{bh^2}{6} f_m \tag{37}$$

The bending moment at bond layer shear failure (a) is denoted $M_{v,b}$. By use of Eq. (31) and (8) or Table 1 is the ratio $M_{v,b}$ to M_m found to be:

$$\frac{M_{v,b}}{M_m} = \frac{h}{b}\sqrt{\frac{a^2}{h^2} + \frac{a^4}{h^4}}\,\frac{f_{v,b}}{f_m} \tag{38}$$

For longitudinal out-of-plane shear stress τ_{xz} in the adherend at the bond interface (b):

$$\frac{M_{v,90}}{M_m} = \frac{h}{b}\left(\frac{a}{h} + \frac{a^3}{h^3}\right)\frac{f_v}{f_m} \tag{39}$$

And for the rolling shear stress τ_{yz} in the adherend at the bond interface (c):

$$\frac{M_{v,r}}{M_m} = \frac{h}{b}\left(1 + \frac{a^2}{h^2}\right)\frac{f_{v,r}}{f_m} \tag{40}$$

For longitudinal in-plane shear stress failure in the adherend (e):

$$\frac{M_{v,0}}{M_m} = \frac{8}{3}\left(\frac{a}{h} + \frac{h}{a}\right)\frac{f_v}{f_m} \tag{41}$$

And for tensile stress perpendicular to grain failure in the adherend (f):

$$\frac{M_{t,90}}{M_m} = 6\sqrt{3}\left(1 + \frac{a^2}{h^2}\right)\frac{f_{t,90}}{f_m} \tag{42}$$

For compressive stress perpendicular to the grain is the corresponding expression valid with $f_{t,90}$ replaced by $f_{c,90}$. For timber is $f_{c,90} > f_{t,90}$ and accordingly is $f_{c,90}$ not decisive.

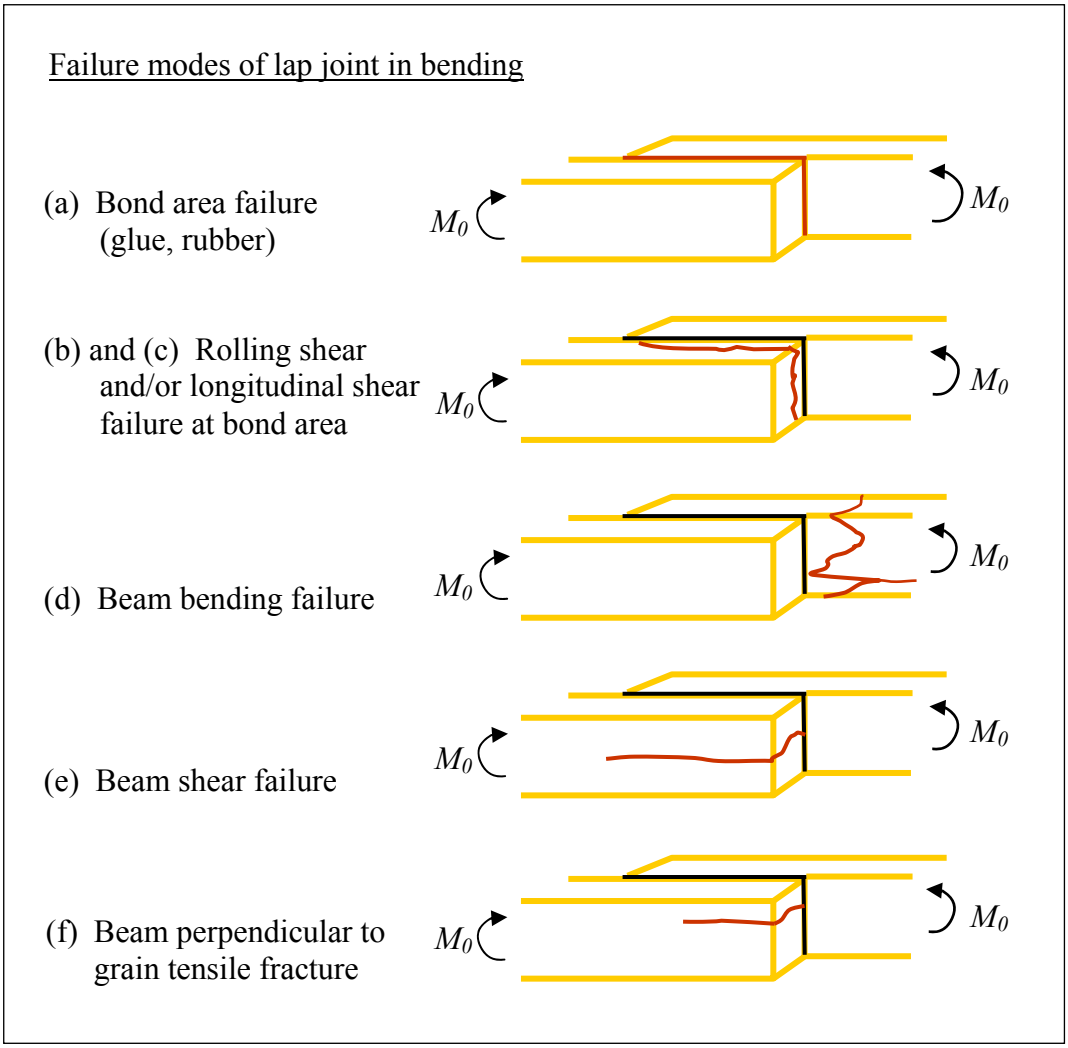

Figure 4. Failure modes of lap joint in bending.

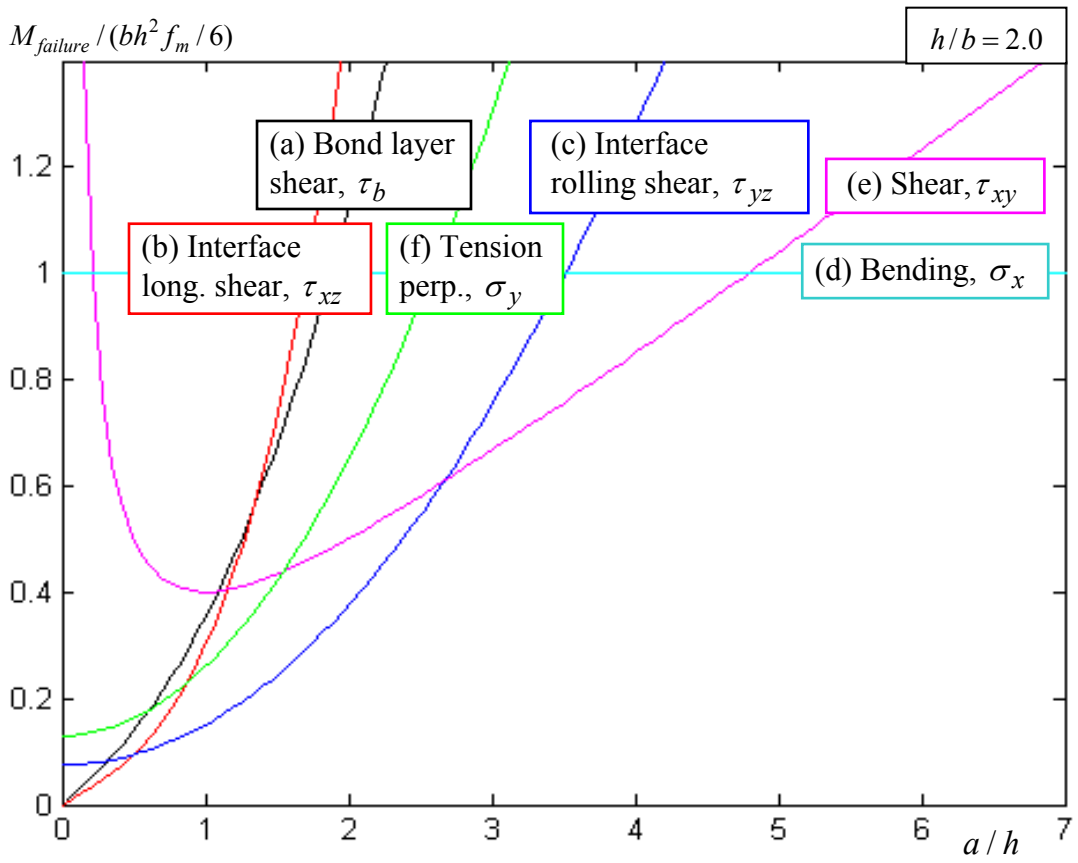

Figure 5. Joint bending moment capacity versus joint length to depth ratio at different failure modes.

To illustrate the bending capacity corresponding to the different failure modes and how the joint capacity is affected by ratios a/h and h/b adherend material parameters corresponding to a quality of glued laminated timber are used. Characteristic strength values for glulam 'L40' are according to the Danish "SBI-anvisning 210 Traekonstruktioner" (Larsen and Riberholt, 2005):

$$f_{m,k} = 40\,MPa$$
$$f_{v,90,k} = f_{v,0,k} = f_{v,k} = 3.0\,MPa$$
$$f_{v,r,k} = 1.5\,MPa$$
$$f_{t,90,k} = 0.5\,MPa$$

where the value of $f_{v,r,k}$, not defined in "SBI-anvisning 210", is made equal to $f_{v,k}/2$ as proposed in "Limträhandbok" (Carling, 2001). Index k indicates characteristic value, i.e. the 5 percentile value. For the bond layer is a shear strength value estimated from recent tests of a glued rubber foil bond:

$$f_{v,b,k} = 5.0\,MPa$$

The bending moment capacity of the joint versus bond area ratio a/h for the different failure modes is shown in Figure 5 for the above material strength parameter values and adherend depth to thickness ratio $h/b = 2.0$. For the very short joints having $a/h \le 0.5$ is the interface longitudinal shear stress in the wood τ_{xz} decisive. For $0.5 < a/h < 2.7$ is the interface rolling shear in the wood decisive and for $2.7 \le a/h < 4.8$ is longitudinal shear in the centre of the wood parts decisive. The joint reached has its full bending moment capacity for $a/h = 4.8$.

Neither bond layer shear failure nor perpendicular to grain tensile failure is predicted for $h/b = 2.0$. If increasing h/b then the bond area related failure modes becomes less important and the tension perpendicular grain failure mode of greater importance. For very thick joints, i.e. for $h/b \le 1.0$, is the rolling shear fracture in wood of predominant importance.

With adherend material data typical for timber and bond layer data typical for a rubber foil, it seems that the required joint length for full bending moment capacity is governed either by rolling shear fracture in the wood close to the bond area (thick joints) or by longitudinal shear fracture within the wood parts.

5.3 Joint bending strength analysis – orthotropic bond layer

A joint exposed only to bending and with an orthotropic bond layer is analyzed. The orthotropic bond layer properties are characterized by β, defined by $\beta = G_{yz}/G_{xz}$.

The full bending moment capacity of the joint is determined by bending failure of the adherends. This moment capacity is given by criteria (d), it is denoted M_m and is not affected by β:

$$M_m = \frac{bh^2}{6} f_m \tag{43}$$

The bending moment at bond layer shear failure, $M_{v,b}$, is determined by (13):

$$\frac{M_{v,b}}{M_m} = \frac{a(\beta a^2 + h^2)}{bh\sqrt{\beta^2 a^2 + h^2}} \frac{f_{v,b}}{f_m} = \frac{h}{b} \frac{(\beta(a/h)^3 + (a/h))}{\sqrt{\beta^2 (a/h)^2 + 1}} \frac{f_{v,b}}{f_m} \tag{44}$$

The bending moment $M_{v,90}$ at longitudinal out-of-plane shear stress failure corresponding to the stress component τ_{xz} is determined by (12):

$$\frac{M_{v,90}}{M_m} = \frac{h}{b}\left(\frac{a}{h} + \beta \frac{a^3}{h^3}\right) \frac{f_v}{f_m} \tag{45}$$

The bending moment $M_{v,r}$ at out-of-plane rolling shear stress failure corresponding to the stress component τ_{yz} is also determined by (12):

$$\frac{M_{v,r}}{M_m} = \frac{h}{b}(1/\beta + \frac{a^2}{h^2})\frac{f_{v,r}}{f_m} \tag{46}$$

The bending moment $M_{v,0}$ at in-plane shear stress failure corresponding to the stress component τ_{xy} is determined by (26):

$$\frac{M_{v,0}}{M_m} = \frac{8}{3}(\frac{a}{h} + \frac{h}{\beta a})\frac{f_v}{f_m} \tag{47}$$

The bending moment $M_{t,90}$ at tensile stress perpendicular to grain failure in the adherend is determined by (29):

$$\frac{M_{t,90}}{M_m} = 6\sqrt{3}(\frac{1}{\beta} + \frac{a^2}{h^2})\frac{f_{t,90}}{f_m} \tag{48}$$

For compressive stress perpendicular to the grain is the corresponding expression valid with $f_{t,90}$ replaced by $f_{c,90}$. For timber is $f_{c,90} > f_{t,90}$ and accordingly is $f_{c,90}$ not decisive in the case of wood adherends.

6. Verification and accuracy study by finite elements

6.1 Introduction

The major assumption made in the determination of bond layer stresses τ_{yz} and τ_{yz} (see Section 2.1) was that of rigid adherends. The major assumption in the determination of the 2D adherend stresses σ_x, σ_y and τ_{xy} (see Section 3.1) was that of linear distribution of σ_x with respect to y.

In the below are the rigid adherend and the linear σ_x assumptions studied by means of plane stress finite element calculations. Results of a dimensional analysis are presented before going to numerical results. The dimensional analysis was made to identify a dimensionless parameter that defines degree of rigidity of the adherends and to enable more general conclusions from the numerical results.

6.2 Dimensionless parameters in stress analysis

A joint as defined in Figure 1a and Figure 2 is studied. The load applied to the joint is with reference to the adherend shown in Figure 2 defined by the magnitude and the distribution of the normal and shear stresses (tractions) acting on the surface ($x=a/2$, y):

$$\begin{cases} \sigma_x(a/2, y) = \sigma_0 \, f_\sigma(y/h) \\ \tau_{xy}(a/2, y) = \sigma_0 \, f_\tau(y/h) \end{cases} \tag{49}$$

where σ_0 is a scalar that defines the magnitude of the load and where f_σ and f_τ are functions that defines the distributions. As an example, pure bending moment loading can be defined by

$$\sigma_0 = 6M_0/(bh^2), \quad f_\sigma(y/h) = -(y/h)/2 \quad \text{and} \quad f_\tau(y/h) = 0 \tag{50}$$

For the rigid adherend beam type of analysis presented in the previous sections are in addition to the load, two dimensionless ratios needed for the calculation of stress in the adherends. These two parameters are the joint shape ratio and the bond layer orthotropic stiffness ratio:

$$\begin{cases} a/h \\ \beta = G_{yz}/G_{xz} \end{cases} \tag{51}$$

All stresses are proportional to σ_0 and the stresses in the bond layer are moreover proportional to ratio (*b/a*). The stresses in a point (*x/a*, *y/h*) can thus be expressed as:

$$\begin{cases} \tau_{xz}/\sigma_0 = (b/a)\, f_{xz}(\beta, a/h) \\ \tau_{yz}/\sigma_0 = (b/a)\, f_{yz}(\beta, a/h) \\ \tau_b/\sigma_0 = (b/a)\, f_b(\beta, a/h) \\ \sigma_x/\sigma_0 = f_x(\beta, a/h) \\ \tau_{xy}/\sigma_0 = f_{xy}(\beta, a/h) \\ \sigma_y/\sigma_0 = f_y(\beta, a/h) \end{cases} \tag{52}$$

Explicit expressions for the functions f_{xz} etc can be obtained from equations (12) and (13), and (22), (26) and (29), respectively.

Leaving the rigid adherend model and instead looking at a model where the adherends are modeled as plane stress linear elastic isotropic plates, two dimensionless ratios have to be added to those in (51):

$$\begin{cases} Eb/(G_{xz}a^2/t) \\ \nu_{xy} \end{cases} \tag{53}$$

The first ratio is a measure of the degree of rigidity of the adherends, *E* being the Young's modulus of the adherend material. The second dimensionless parameter, υ, is the Poisson's ratio of the adhered material. For an orthotropic adherend material the number of additional parameters is four:

$$\begin{cases} E_x b/(G_{xz}a^2/t) \\ \nu_{xy} \\ E_x/E_y \\ E_x/G_{xy} \end{cases} \tag{54}$$

E_x is a measure of the magnitude of the stiffness of the orthotropic material. For an isotropic material is $E_x=E$.

Finally, the stresses in a point (*x/a*, *y/h*) in a joint made up of orthotropic adherends and an orthotropic bond layer are found to be determined by dimensionless ratios according to:

$$\begin{cases} \tau_{xz}/\sigma_0 = (b/a)\, f_{xz}(\beta, a/h, E_x b/(G_{xz}a^2/t), \nu_{xy}, E_x/E_y, E_x/G_{xy}) \\ \tau_{yz}/\sigma_0 = (b/a)\, f_{yz}(\beta, a/h, E_x b/(G_{xz}a^2/t), \nu_{xy}, E_x/E_y, E_x/G_{xy}) \\ \tau_{b}/\sigma_0 = (b/a)\, f_{b}(\beta, a/h, E_x b/(G_{xz}a^2/t), \nu_{xy}, E_x/E_y, E_x/G_{xy}) \\ \sigma_x/\sigma_0 = f_x(\beta, a/h, E_x b/(G_{xz}a^2/t), \nu_{xy}, E_x/E_y, E_x/G_{xy}) \\ \tau_{xy}/\sigma_0 = f_{xy}(\beta, a/h, E_x b/(G_{xz}a^2/t), \nu_{xy}, E_x/E_y, E_x/G_{xy}) \\ \sigma_y/\sigma_0 = f_y(\beta, a/h, E_x b/(G_{xz}a^2/t), \nu_{xy}, E_x/E_y, E_x/G_{xy}) \end{cases} \quad (55)$$

6.3 Finite element model and calculated stress distributions

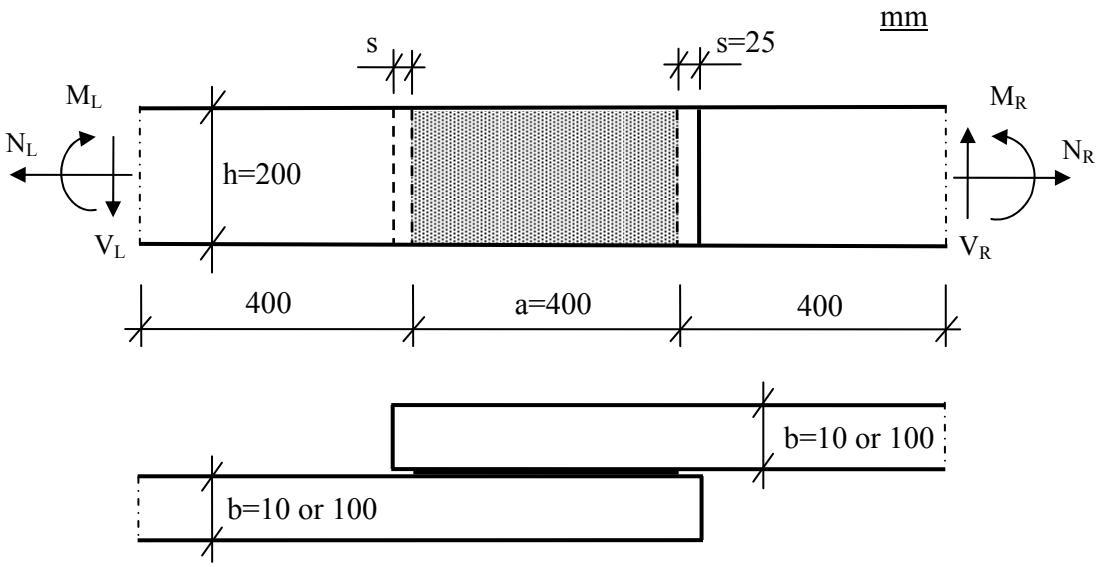

Figure 6. Joint analyzed by finite elements.

A joint with geometry according to Figure 6 is analyzed. The finite element model is made up of 4-node plane stress plate elements of the Melosh type, overlapping in the joint area and with internodal springs modeling the shear layer. The plate element size is 5x5 mm^2. Not glued end-parts of length s=25 mm were added to avoid stress-irregularities at bonded edges found at plane stress analysis. The model was built in the Calfem/Matlab computer program.

Seven FE-analyses are presented. In order to study the influence of the linear σ_x assumption separately, first three analysis were made with high values of the adherend rigidity ratio $E_x b/(G_{xz}a^2/t)$. Then two analyses corresponding to adherends made of steel and wood, respectively, are presented.

These five analyses relate to pure bending of the joint. Analyses number six and seven relates to a loading that give pure shear force at the centre of the joint. The magnitude of the bending load corresponds to beam bending stress 40.0 MPa for adherend width 100 mm, and the shear force load corresponds to beam shear stress 3.0 MPa for the same adhered width.

Input data for the seven analyses are given in Table 1. Corresponding stress calculations were made by the rigid adherend beam model.

The material and thickness data for the bond layer corresponds roughly to that of a thin rubber mat glued in between the two adherends. The lower value, 0.33 MPa, for G_{yz} used in the calculation representing wood corresponds to consideration to the low rolling shear stiffness of wood: it can be reasonably to include the out-of-plane shear compliance of the adherend when assigning a shear stiffness value to the bond layer. An equivalent value of bond layer shear stiffness, $G_{yz,eqv}$, can be approximately estimated by adding compliances of the bond layer and the two adherends, regarded as being exposed to the full shear stress from the loaded surface to the centre of the adherend:

$$\frac{t}{G_{yz,eqv}} = \frac{t}{G_{yz,bond}} + \frac{b/2}{G_{yz,adherend}} + \frac{b/2}{G_{yz,adherend}} \tag{56}$$

With t=1.0 mm, $G_{yz,bond}$ = 1.0 MPa, b=100 mm and $G_{yz,adherend}$ = 50 MPa, $G_{yz,eqv}$ becomes equal to 0.33 MPa.

The seven pages after Table 1 shows the finite element model computational results on the right hand side and on the left hand side the corresponding results of the rigid adherend beam type of model.

Calculations 1-3 suggest that the bond layer stresses obtained by the rigid adherend model coincide with those obtained by the finite element model for joints with high adherend stiffness ratio $E_x bt/(Ga^2)$. The calculated adherend stresses suggests that the assumption of linear σ_x with respect to y has very little influence on σ_x and τ_{xy}. The calculated magnitude and distribution of σ_y is somewhat affected.

Calculation no 4 compared to calculation no 1 suggests that the performance of a possible typical steel-rubber-steel lap joint is almost identical to the performance of a rigid adherend joint type of joint. Calculation no 5 compared to no 3 suggests that the performance of a typical wood-rubber-wood lap joint is affected by the deformations in the wood. For the bond layer shear stress is stress concentration to the corners of the bond area found. Also the adherend stresses σ_x, τ_{xy} and σ_y are affected, although not as much as the bond shear stress.

Calculations no 6 and 7 relate to the stresses at shear force loading. For the steel type of joint are about the same stresses found by the rigid adherend model as by the finite element model. For the wood type of joint some deviations can be seen. The stresses produced by

shear force loading are in general small and the conventional beam shear stress in the close vicinity of the joint is probably, in most cases, decisive for the load capacity.

Table 1. Material, thickness and load data used in FE-calculations.

Calculation no Bond/Adherend Bond/Adherend	FE-1 Rubb./Rigid Iso./Iso.	FE-2 Rubb./Rigid Orth./Iso.	FE-3 Rubb./Rigid Orth./Orth.
G_{xz}, MPa	1.0	1.0	1.0
G_{yz}, MPa	1.0	0.33	0.33
t, mm	1.0	1.0	1.0
E_x, MPa	$210000*10^5$	$210000*10^5$	$12000*10^5$
E_y, MPa	Isotropic	Isotropic	$400*10^5$
G_{xy}, MPa	Isotropic	Isotropic	$750*10^5$
υ_{xy}	0.3	0.3	0.0167
b, mm	10	10	100
Load M_R, kNm	26.67	26.67	26.
Load V_R, kN	0	0	0
$E_x bt/(G_{xz}a^2)$	$13.1*10^5$	$13.1*10^5$	$7.5*10^5$

Calculation no Bond/Adherend Bond/Adherend	FE-4 Rubb./Steel Iso./Iso.	FE-5 Rubb./Wood Orth./Orth.	FE-6 Rubb./Steel Iso./Iso.	FE-7 Rubb./Wood Orth./Orth.
G_{xz}, MPa	1.0	1.0	1.0	1.0
G_{yz}, MPa	1.0	0.33	1.0	0.33
t, mm	1.0	1.0	1.0	1.0
E_x, MPa	210000	12000	210000	12000
E_y, MPa	Isotropic	400	Isotropic	400
G_{xy}, MPa	Isotropic	750	Isotropic	750
υ_{xy}	0.3	0.0167	0.3	0.0167
b, mm	10	100	10	100
Load M_R, kNm	26.67	26.67	-12.0	-12.0
Load V_R, kN	0	0	20.0	20.0
$E_x bt/(G_{xz}a^2)$	13.1	7.5	13.1	7.5

Pure bending M_0=26.67 kNm, isotropic bond layer β=1.0

Rigid adherend beam analysis

FE-analysis FE-1
Isotropic, almost rigid adherend

τ_b, N/mm^2

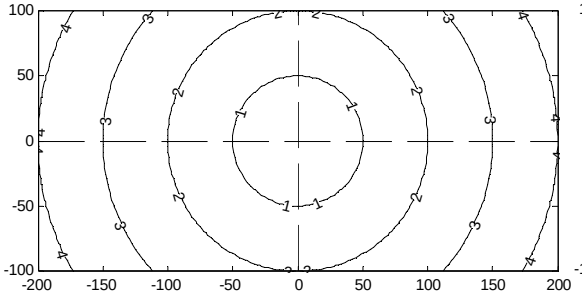

τ_b, N/mm^2

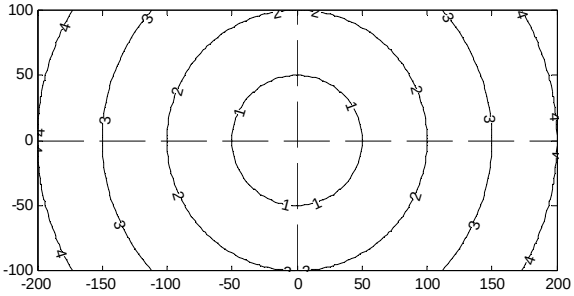

σ_x, N/mm^2

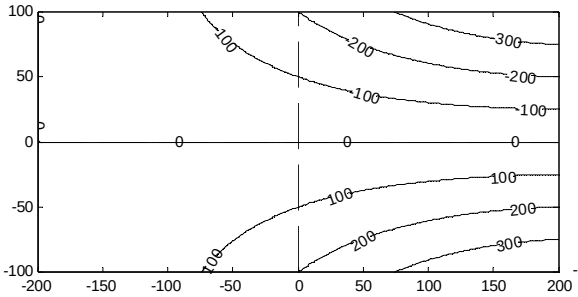

σ_x, N/mm^2

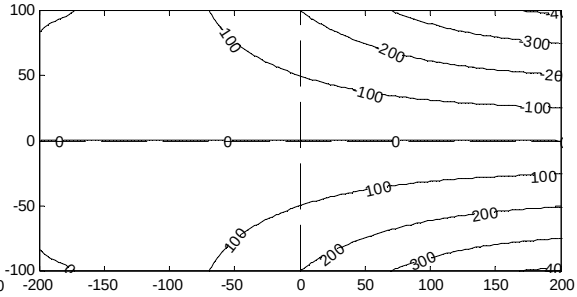

τ_{xy}, N/mm^2

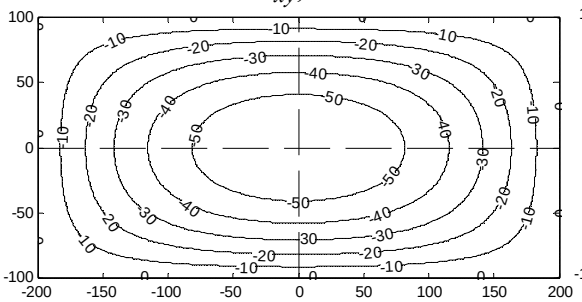

τ_{xy}, N/mm^2

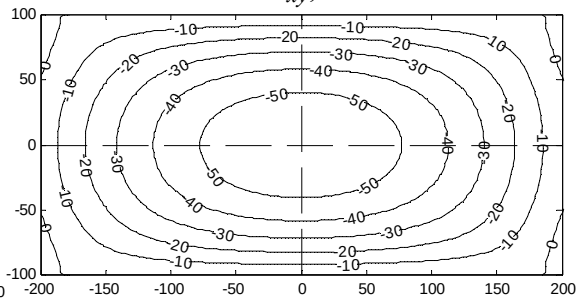

σ_y, N/mm^2

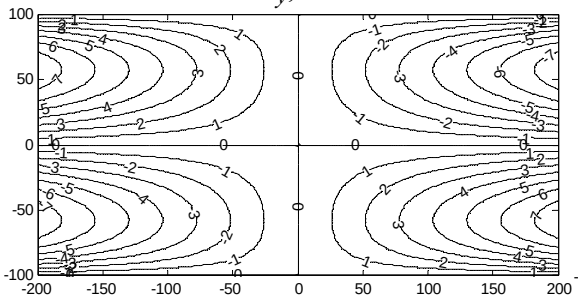

σ_y, N/mm^2

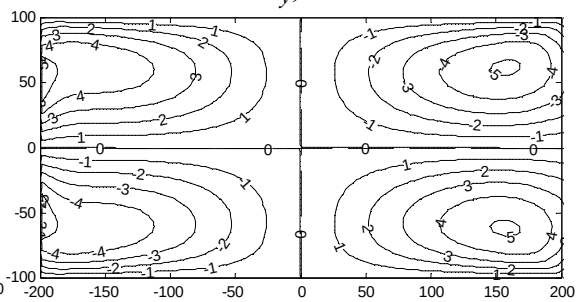

Pure bending M_0=26.67 kNm, orthotropic bond layer β=0.33

Rigid adherend beam analysis

FE-analysis FE-2
Isotropic, almost rigid adherend

τ_b, N/mm^2

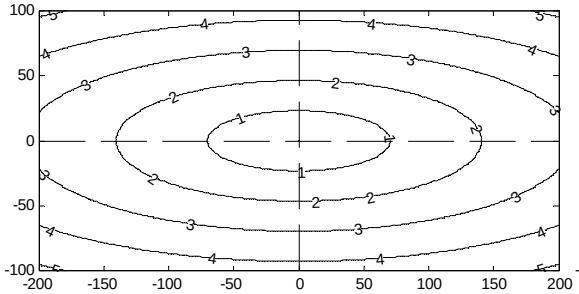

τ_b, N/mm^2

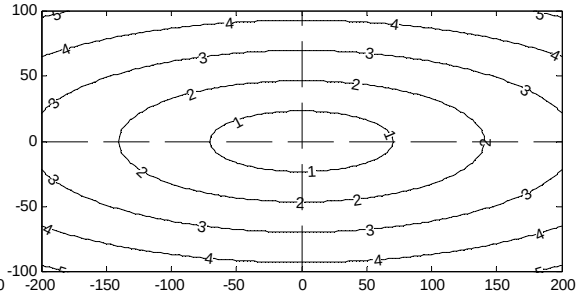

σ_x, N/mm^2

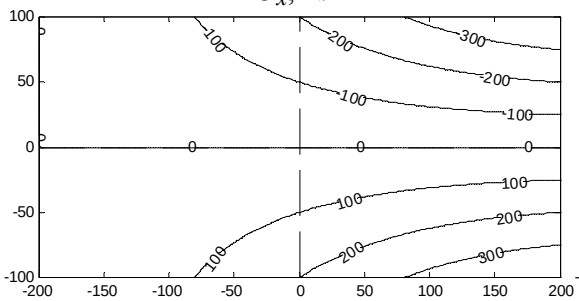

σ_x, N/mm^2

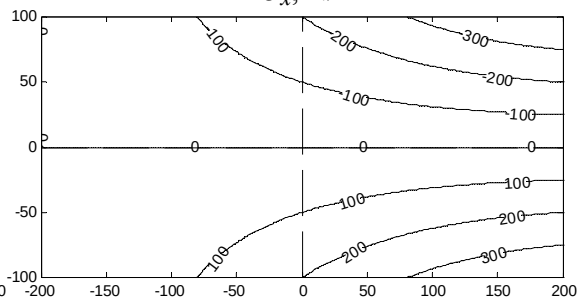

τ_{xy}, N/mm^2

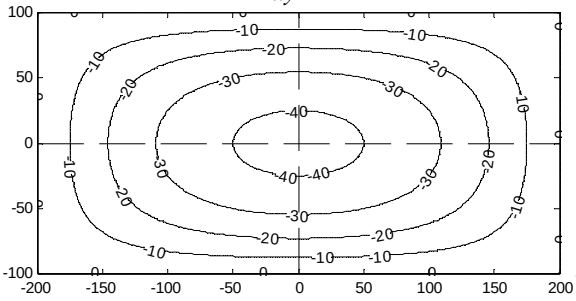

τ_{xy}, N/mm^2

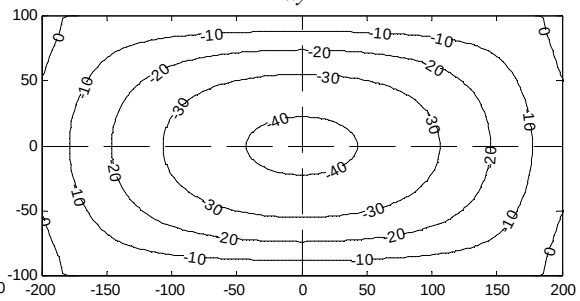

σ_y, N/mm^2

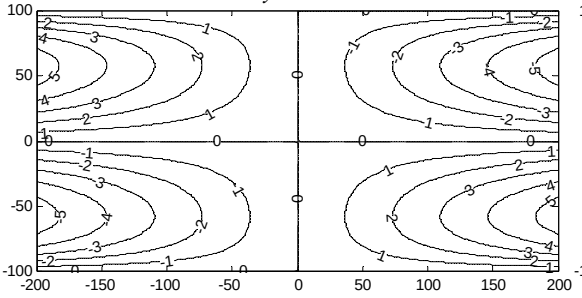

σ_y, N/mm^2

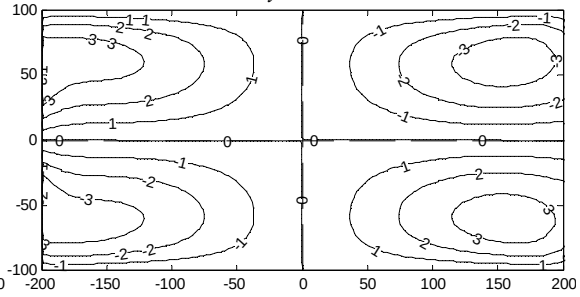

Pure bending M_0=26.67 kNm, orthotropic bond layer β=0.33

Rigid adherend beam analysis

FE-analysis FE-3
Orthotropic, almost rigid adherend

τ_b, N/mm^2

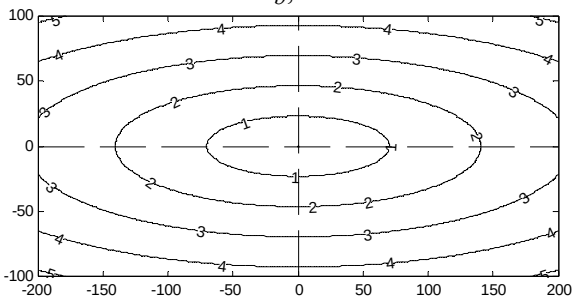

τ_b, N/mm^2

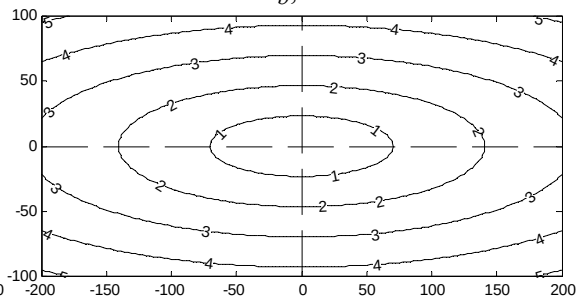

σ_x, N/mm^2

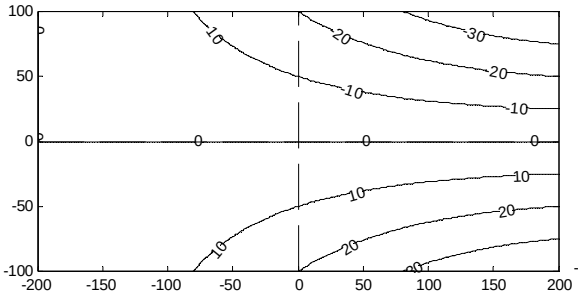

σ_x, N/mm^2

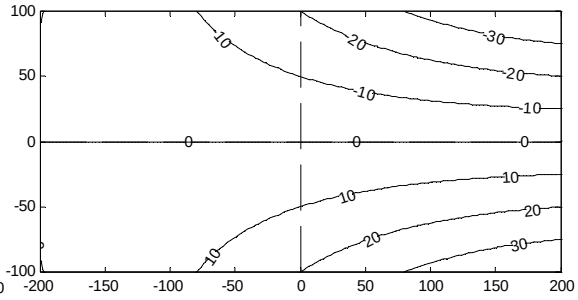

τ_{xy}, N/mm^2

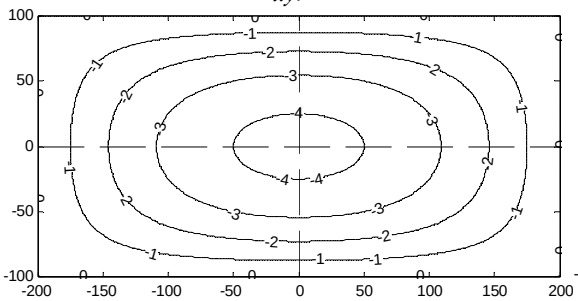

τ_{xy}, N/mm^2

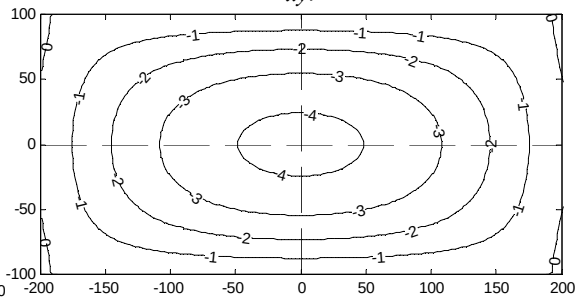

σ_y, N/mm^2

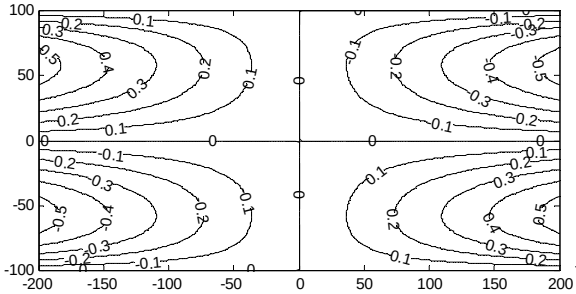

σ_y, N/mm^2

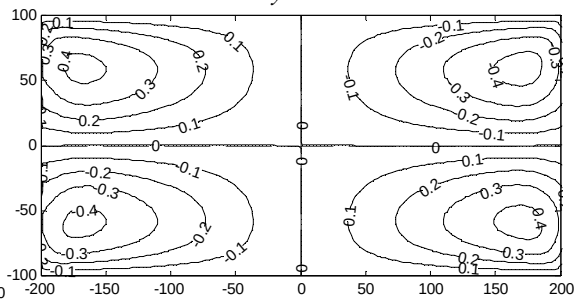

Pure bending M_0=26.67 kNm, isotropic bond layer β=1.0

Rigid adherend beam analysis

FE-analysis FE-4
Isotropic steel adherend

τ_b, N/mm^2

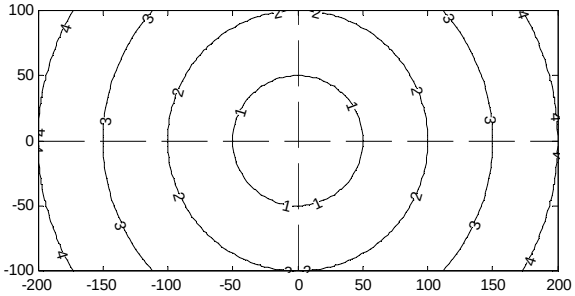

τ_b, N/mm^2

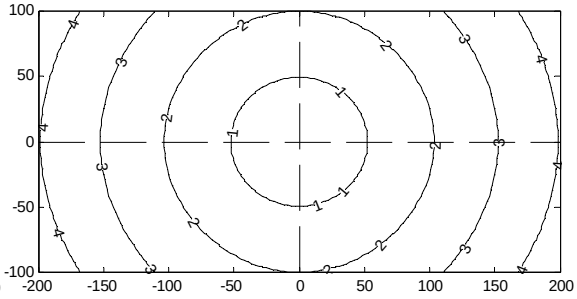

σ_x, N/mm^2

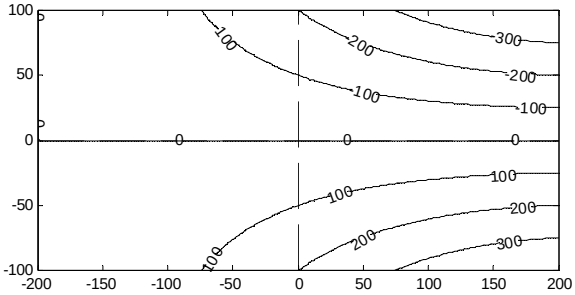

σ_x, N/mm^2

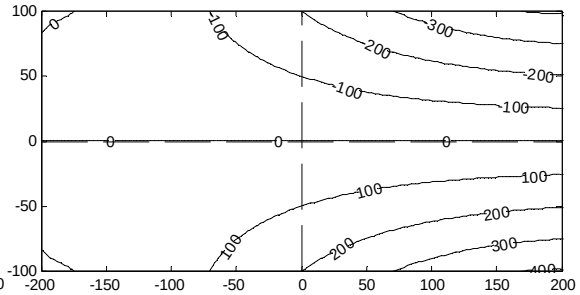

τ_{xy}, N/mm^2

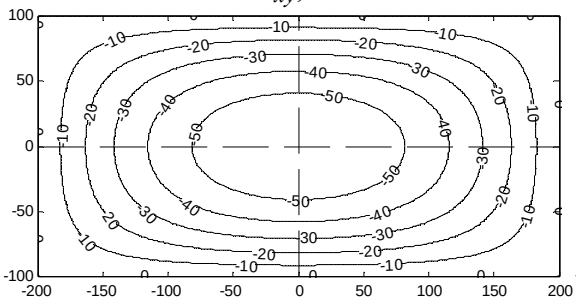

τ_{xy}, N/mm^2

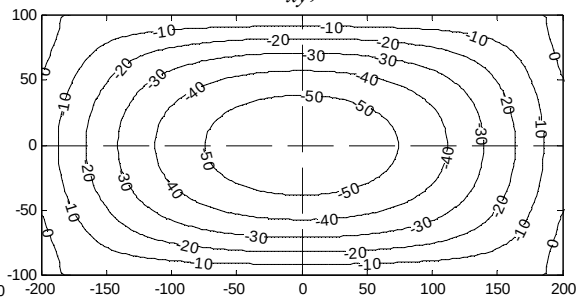

σ_y, N/mm^2

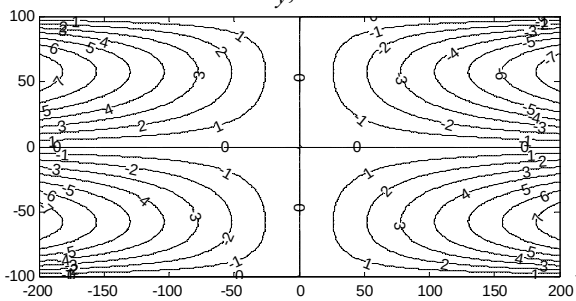

σ_y, N/mm^2

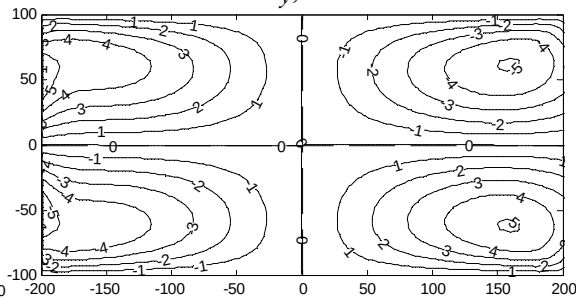

Pure bending M_0=26.67 kNm, orthotropic bond layer β=0.33

Rigid adherend beam analysis

FE-analysis FE-5
Orthotropic wood adherend

τ_b, N/mm^2

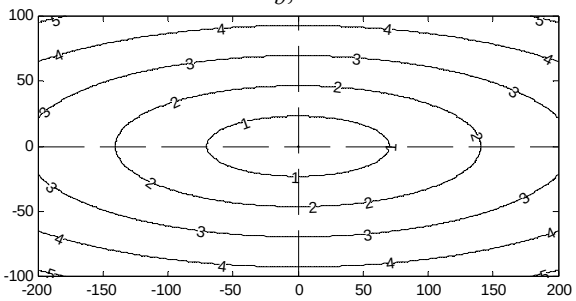

τ_b, N/mm^2

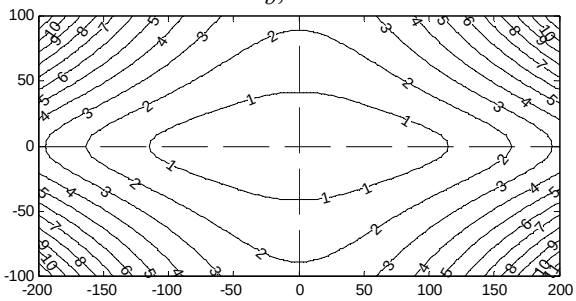

σ_x, N/mm^2

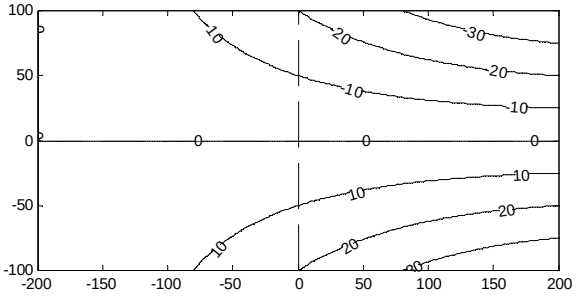

σ_x, N/mm^2

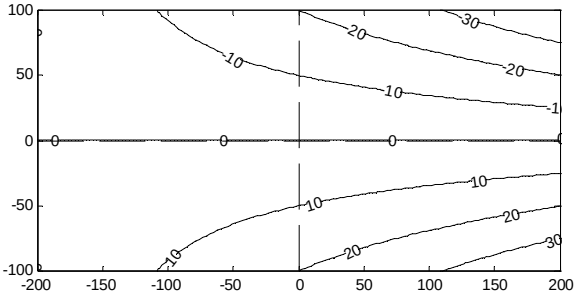

τ_{xy}, N/mm^2

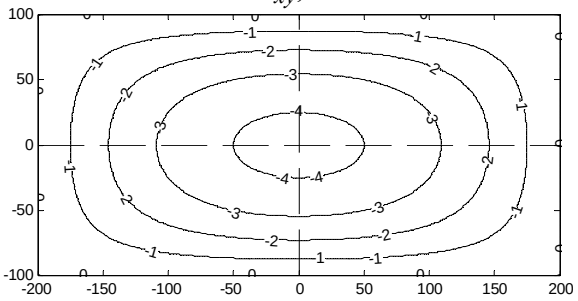

τ_{xy}, N/mm^2

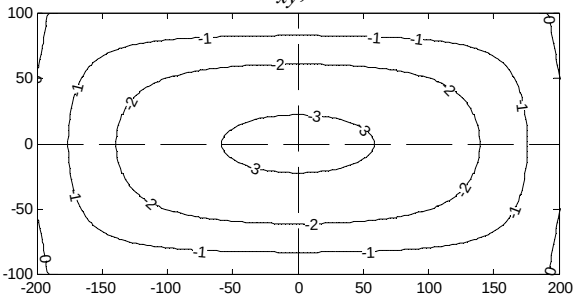

σ_y, N/mm^2

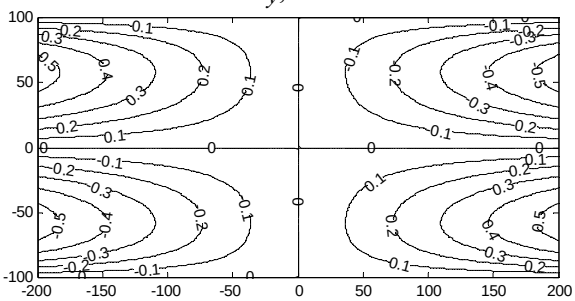

σ_y, N/mm^2

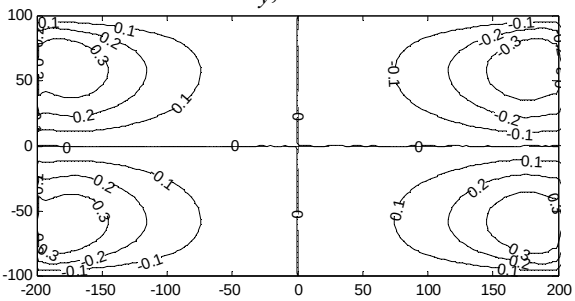

Shear loading V_0=40 kN, M_0= -8.0 kNm, isotropic bond layer β=1.0

Rigid adherend beam analysis

FE-analysis FE-6
Isotropic steel adherend

τ_b, N/mm^2

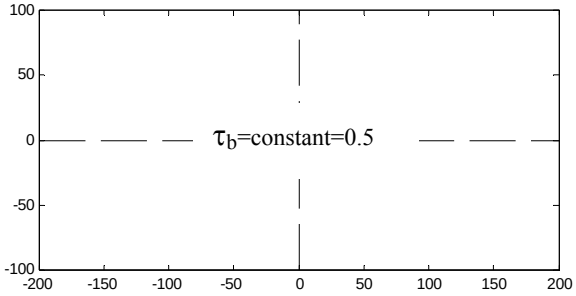

τ_b, N/mm^2

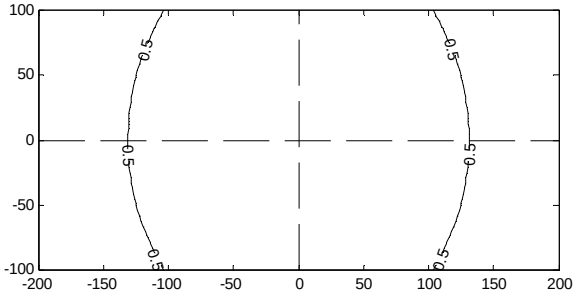

σ_x, N/mm^2

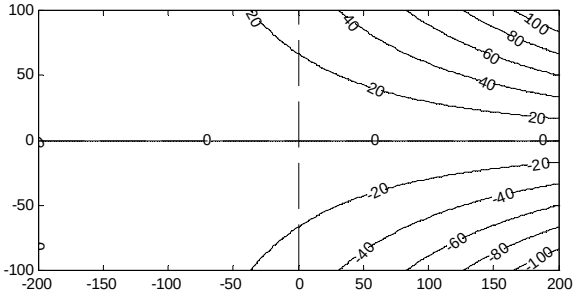

σ_x, N/mm^2

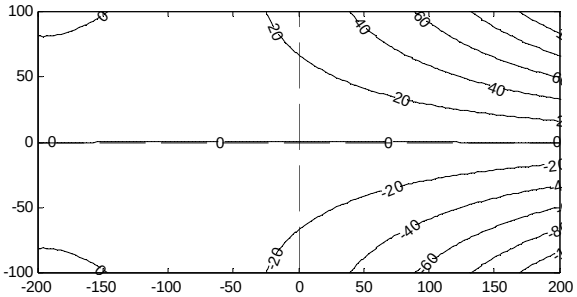

τ_{xy}, N/mm^2

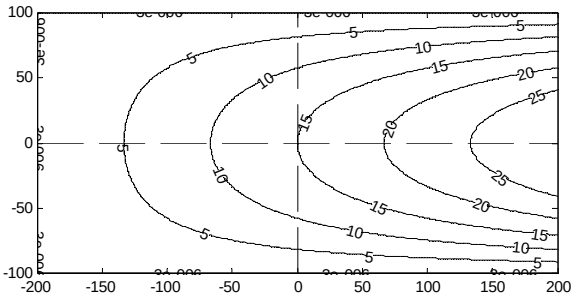

τ_{xy}, N/mm^2

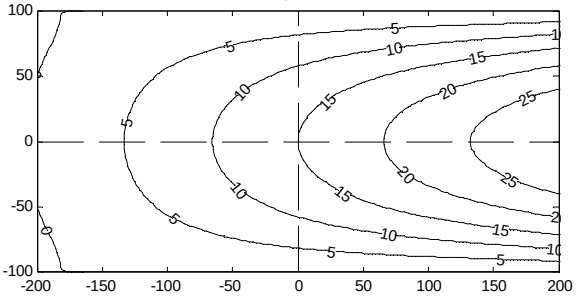

σ_y, N/mm^2

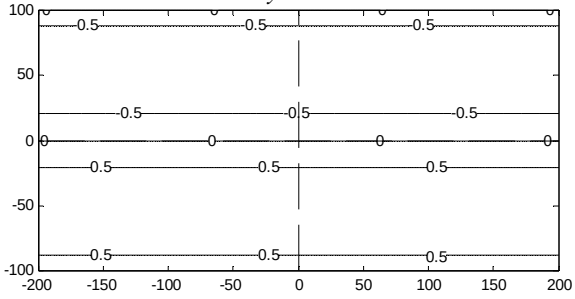

σ_y, N/mm^2

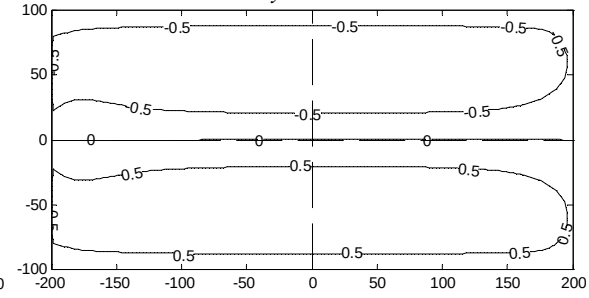

Shear loading V_0=40 kN, M_0= -8.0 kNm, orthotropic bond layer β=0.33

Rigid adherend beam analysis

FE-analysis FE-7
Orthotropic wood adherend

τ_b, N/mm^2

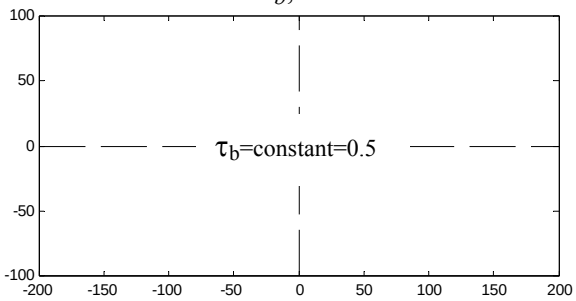

τ_b, N/mm^2

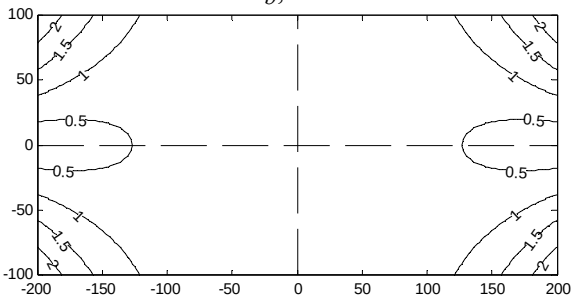

σ_x, N/mm^2

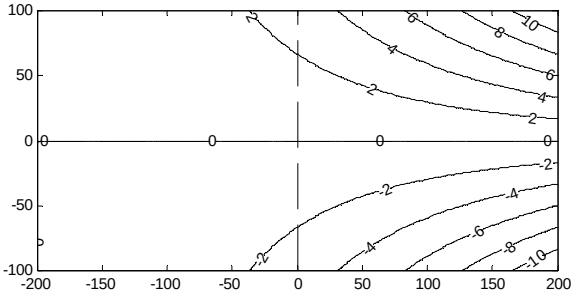

σ_x, N/mm^2

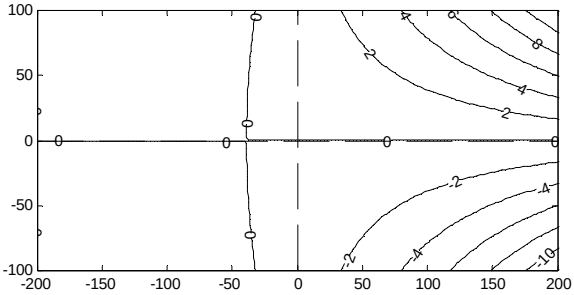

τ_{xy}, N/mm^2

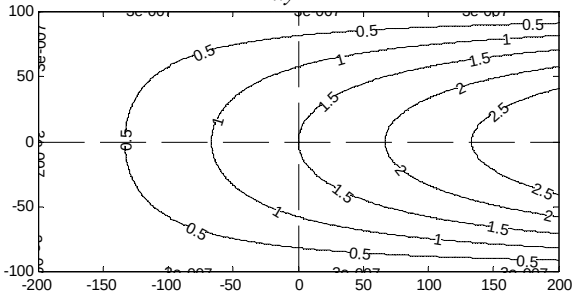

τ_{xy}, N/mm^2

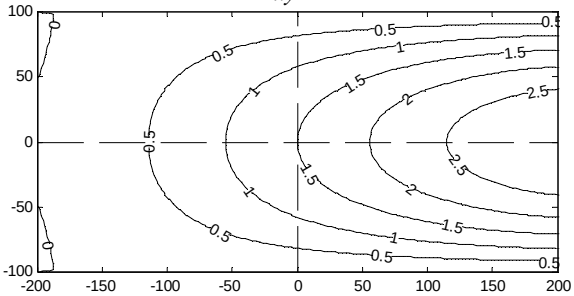

σ_y, N/mm^2

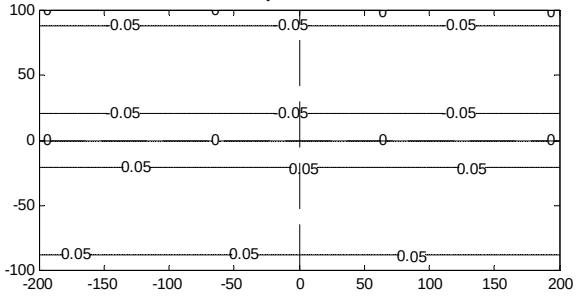

σ_y, N/mm^2

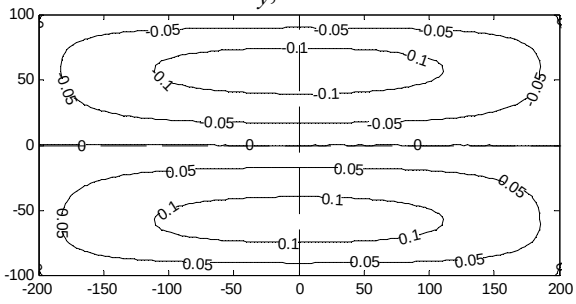

6.4 Influence of adherend stiffness ratio $Ebt/(Ga^2)$

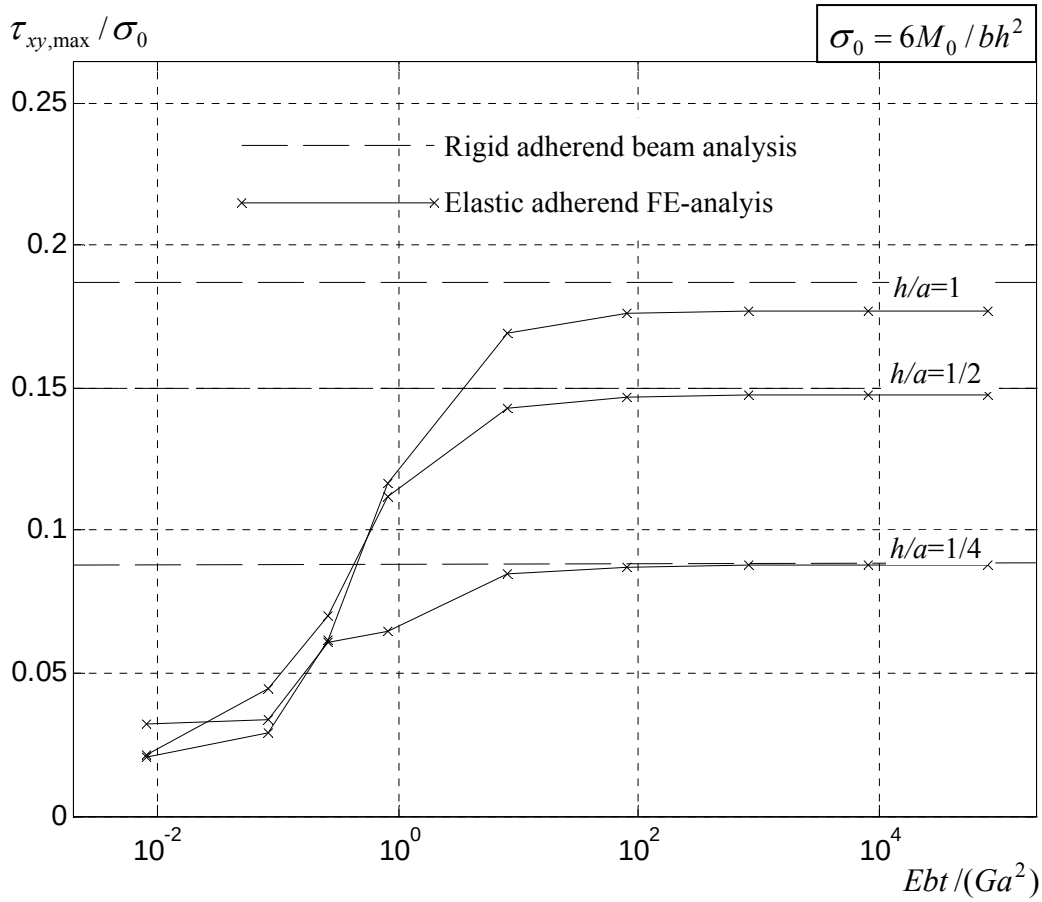

Figure 7. Maximun shear stress $\tau_{xy,\max}$ in adherend versus adherend stiffness ratio $Ebt/(Ga^2)$ for a joint loaded by a bending moment M_0 and made up of isotropic adhedrends (ν=0.3) and an isotropic bond layer.

The influence of the adheren stiffnes ratio is studied by calculating the maximum of the adherend shear stress τ_{xy} for various values of $Ebt/(Ga^2)$ for joints made up of isotropic adherend and bond layer materials, and loaded by a bending moment, $M_0=\sigma_0 bh^2/6$. To be more precise, following Eq. (55), ratio $\tau_{xy,max}/\sigma_0$ is calculated for β=1, h/a=1/4, 1/2 and 1/1, various $Ebt/(Ga^2)$, υ=0.3, E_x/E_y=1 and E_x/G_{xy}= 2(1+υ).

The computational results are shown in Figure 7. It seems that $\tau_{xy,max}$ is affected by the adherend stiffness ratio for values of $Ebt/(Ga^2)\leq 10$. For $Ebt/(Ga^2)\leq 1$ there is a very evident influence. As $Ebt/(Ga^2)$ approaches zero, one may expect a plane stress model to predict zero $\tau_{xy,\max}$.

Figure 8 shows that not only the magnitude of the stresses, but also the overall distribution of the stresses changes when the adherend stiffness ratio is decreased from about 10 and downwards.

The present example relates to an isotropic material. An approximate estimation of the corresponding approximate shift-values for $Ebt/(Ga^2)$ for an orthotropic adherend material and/or an orthotropic bond layer material can be obtained by replacing E with $\sqrt{E_x E_y}$ and G with $\sqrt{G_{xz} G_{yz}}$, respectively. For wood-rubber-wood joints this suggests that the rigid adherend model can give accurate stress predictions in some cases, e.g. for joints with small length a, but not always.

If using the rigid adherend model in stress analysis of joints with compliant adherends and exposed to bending, it seems that the maximum bond layer shear stress τ_b in general will be underestimated, the maximum adherend stress σ_x will be slightly underestimated, the adherend shear stress τ_{xy} somewhat overestimated and also the adherend normal stress σ_y somewhat overestimated.

For a joint exposed to shear force loading, the same trends are found expect for σ_y for which the rigid adherend model give an underestimation. For a joint exposed to normal force loading, application of the rigid adherend model to a joint with compliant adherends will give underestimation of the maximum bond layer shear stress. The influence on the maximum of the adherend stresses σ_x will be zero or very small. Maximum of τ_{xy} and σ_y will in general be of minor interest since these stress components can be expected to be zero or very small for the normal force loading of the joint.

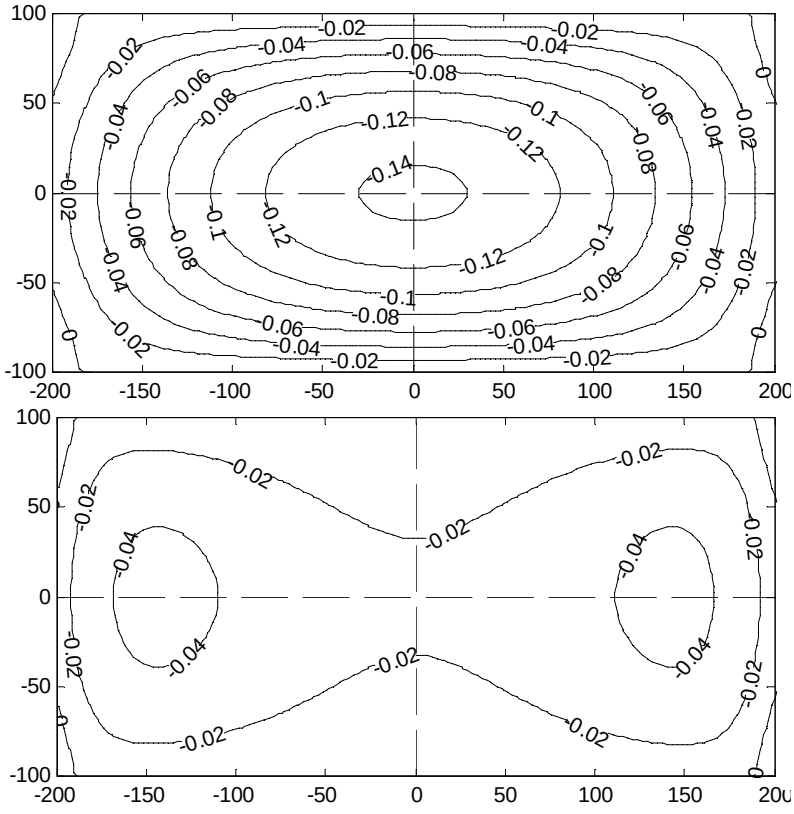

a) $Ebt/(Ga^2)=8.0$

b) $Ebt/(Ga^2)=0.08$

Figure 8. Shear stress τ_{xy}/σ_0 in a stiff adherend, a), and in a compliant adherend, b).

7. Concluding remarks

In strength design of joints attention is commonly attracted to the capacity of the joining device, e.g. a glue bond line or dowels. However, in some cases, or perhaps even in many cases, the stresses in the adherend material are decisive for the capacity of the joint. This is the case when the joining device has large load capacity as compared to the strength of the adherend material. An example is joining of timber structural elements by means rubber foil glue joints. To get a possibility to estimate the stresses not only in the bond layer, but also in the adherend material explicit stress equations were developed by assuming a rigid performance of the adherends. Comparison to results of planes stress finite element analyses showed good results for joints with high adherend rigidity ratio $Ebt/(Ga^2)$. Timber rubber foil adhesive joints are typically in an order of magnitude between high and low values of the rigidity ratio. This implies the need for a calculation model where the deformation of the adherend material is considered. One such model is the plane stress finite element model, which, however, has the drawback of not allowing simple explicit stress equations. Another possibility is modeling of the deformation of the adherends with a beam theory model. Using the Timoshenko beam theory, this leads to a set of 6 homogeneous differential equations with 6 unknown scalar functions of the length coordinate x. It is unfortunate that theses equations probably lead to stress equations that are comprehensive, although perhaps explicit.

Acknowledgements

The work presented in this report was carried as a part of the work in a subtask on rubber foil adhesive joints in the joint Swedish-Finnish project “Innovative design, a new strength paradigm for joints, QA and reliability for long-span wood construction”. This 3 year project ongoing 2004-2007 is in turn a part of the "Wood Material Science and Engineering Research Programme" ("Wood Wisdom") and it has been supported by the following organisations and companies.

In Finland:
- TEKES (Finnish Funding Agency for Technology and Innovation)
- VTT
- SPU Systems Oy
- Metsäliitto Cooperative
- Versowood Oyj
- Late-Rakenteet Oy
- Exel Oyj

In Sweden:
- Vinnova (Swedish Governmental Agency for Innovation Systems)
- Skogsindustrierna
- Casco Products AB
- SFS-Intec AB
- Limträteknik i Falun AB
- Svenskt Limträ AB
- Skanska Teknik AB

The contributions and funding from the above mentioned parties are gratefully acknowledged. Thanks also to tech. lic. Lena Strömberg for check of equations.

January 2008, Per Johan Gustafsson

References

Björnsson, P. and Danielsson, H., 2005: “Strength and creep analysis of glued rubber foil timber joints”, Master thesis, Report TVSM-5137, Division of Structural Mechanics, Lund University, Sweden, pp 93

Carling, O., 2001: ”Limträhandbok”, Svenskt Limtä AB, Sverige, pp 232

Gustafsson, P.J., 2006: “A structural joint and support finite element”, Report TVSM 7143, Division of Structural Mechanics, Lund University, Sweden, pp 43.

Gustafsson, P.J., 2007: ”Tests of full size rubber foil adhesive joints”, Report TVSM-7149, Division of Structural Mechanics, Lund University, Sweden, pp 97

Larsen, H.J. and Riberholt, H., 2005: “Traekonstruktioner. Beregning”, SBI-anvisning 210, Statens Byggeforskningsinstitut, Danmark, pp 216